THE ASTROPHYSICAL JOURNAL, 453:792–809, 1995 November 10

NEUTRINO CAPTURE AND SUPERNOVA NUCLEOSYNTHESIS

GEORGE M. FULLER[1] AND BRADLEY S. MEYER[2]
Received 1994 October 21; accepted 1995 May 18

ABSTRACT

We investigate charged current neutrino and antineutrino capture on nuclei in the post–core bounce supernova environment. We point out that these processes may play an important, and heretofore overlooked, role in determining the nucleosynthesis in models of neutrino-heated supernova ejecta. In particular, we suggest that inclusion of these rates may help solve the problem in these models of overproduction of nuclides with neutron numbers near 50 and, in addition, enhance the production of the some of the light *p*-process nuclei in the α-process, particularly ^{92}Mo. The neutrino capture rates on neutron-rich nuclei are found to be dominated by transitions to the Fermi (isobaric analog state) and Gamow-Teller resonances. In these cases, the neutrino capture thresholds are approximately just the nuclear Coulomb energy differences between nuclear parents and daughters, and the neutrino capture rates therefore exhibit only weak dependence on neutron and proton numbers compared to that of β^--decay rates. We exploit this property to constrain the location of the *r*-process region in the post–core bounce supernova environment. We present analytic estimates for the rates of electron neutino and antineutrino capture on nuclei and nucleons.

Subject headings: elementary particles — nuclear reactions, nucleosynthesis, abundances — stars: interiors — supernovae: general

1. INTRODUCTION

In this paper we examine the physics of charged current electron neutrino and antineutrino capture on heavy nuclei in the region above the neutrino sphere in models of the post–core bounce Type II supernova environment. Our results suggest that proper inclusion of these rates in computations of nucleosynthesis in neutrino-heated supernova ejecta may help provide the solution to the problem in these models of overproduction of isotopes in the vicinity of the closed shell at neutron number $N = 50$. In turn, this work leads us to propose that charged current electron neutrino capture on heavy nuclei helps the α-process (Woosley & Hoffman 1992), occurring in neutrino-heated ejecta $\sim$0.5–1 s after core bounce, to produce the bulk of the solar system's supply of ^{92}Mo. While our speculations on neutrino capture during the α-process are new, the general notion that neutrino captures might play a role in the synthesis of *p*-nuclei is fairly old (Domogatsky & Nadyozhin 1977). In addition, we employ our neutrino capture rates to place important constraints on the location and/or outflow velocity of the *r*-process synthesis site.

Recently there has been a revolution in our understanding of the role neutrinos play, both in late-time Type II supernova dynamics (see Bethe & Wilson 1985; Herant, Benz, & Colgate 1992; Miller, Wilson, & Mayle 1993; Burrows & Fryxell 1993), and in heavy element nucleosynthesis from neutrino-heated material ejected after the supernova explosion (Haxton 1987; Woosley et al. 1990; Woosley & Hoffman 1992; Meyer et al. 1992; Takahashi, Witti, & Janka 1994; Woosley et al. 1994). In particular, neutrinos may be instrumental in reviving the stalled shock at times of order $t_{pb} < 1$ s (hereafter t_{pb} denotes the time post–core bounce). Neutrinos carry away of order 99% of the gravitational binding energy of the proto–neutron star formed following core collapse. Ultimately, these neutrinos *cause* the supernova explosion, through a combination of direct heating of the material above the neutron star and induced convection. In addition, the nucleosynthesis from the material ejected during and after this explosion process is largely determined by neutrino interactions.

Matter that is initially in nuclear statistical equilibrium (NSE) near the neutrino sphere will eventually "freeze out" of equilibrium as it moves out to larger radii where the temperature is lower. The nucleosynthesis produced in such a freezeout from NSE depends in large measure on three quantities: the neutron-to-proton ratio; the entropy per baryon; and the material expansion rate (e.g., Meyer 1993). In turn, all three of these key nucleosynthesis determinants are set by neutrino interactions.

The entropy per baryon and the material expansion rate depend on the time-integrated history of neutrino neutral current and charged current interactions in the hot plasma above the neutron star. Well after the explosion process, at fairly late times ($t_{pb} > 3$ s), enough neutrino energy has been deposited that the entropy per baryon, *s*, in units of the Boltzmann constant, *k*, may be quite large, $s/k \approx 400$ (see Woosley et al. 1994), and the hydrodynamic outflow of material resembles a neutrino-driven "wind" (Duncan, Shapiro, & Wasserman 1986).

This entropy is large enough that in NSE most baryons reside outside of nuclei. Furthermore, at large enough radius the local plasma temperature is small compared to the temperatures which characterize the ν_e and $\bar{\nu}_e$ distribution functions. In this case, the local neutron-to-proton ratio is set by the competition between $\bar{\nu}_e$ capture on free protons and ν_e capture on free neutrons (Woosley & Baron 1992; Qian et al. 1993):

$$\nu_e + n \rightarrow p + e^- , \tag{1a}$$

$$\bar{\nu}_e + p \rightarrow n + e^+ . \tag{1b}$$

Since the neutron star is sufficiently de-leptonized at this epoch to ensure neutron excess in the material near the neu-

[1] Department of Physics, University of California, San Diego, La Jolla, CA 92093-0319.
[2] Department of Physics and Astronomy, Clemson University, Clemson, SC 29634.

trino sphere, the charged current opacities for ν_e from the process in equation (1a) will exceed those for $\bar{\nu}_e$ from the process in equation (1b). As a result, the $\bar{\nu}_e$ will decouple deeper in the core than do the ν_e, and so the average energies for $\bar{\nu}_e$ will exceed those for ν_e. Typical average neutrino energies at this epoch are $\langle \epsilon_{\bar{\nu}_e} \rangle \approx 16$ MeV for $\bar{\nu}_e$, and $\langle \epsilon_{\nu_e} \rangle \approx 11$ MeV for ν_e (see Qian et al. 1993).

The disparity in energies between $\bar{\nu}_e$ and ν_e is sufficiently large at this epoch that the reactions in equations (1a) and (1b) will drive the material quite neutron-rich. Numerical calculations show that the electron fraction, or net number of electrons per baryon, Y_e, at $t_{pb} > 3$ s can be as low as $Y_e \approx 0.42$. The electron fraction is related to the ratio of net neutron density to net proton density, n/p, by

$$\frac{n}{p} = \frac{1}{Y_e} - 1 \, . \tag{2}$$

The neutron-rich conditions engendered by electron neutrino and antineutrino captures on free nucleons make the neutrino-driven wind after $t_{pb} > 3$ s an apparently ideal site for r-process nucleosynthesis. Calculations of nucleosynthesis from this site by Meyer et al. (1992), Takahashi et al. (1994), and Woosley et al. (1994) give heavy element r-process abundance yields which are in excellent agreement with solar system abundances.

However, a generic feature of these nucleosynthesis calculations seems to be the overproduction by factors as much as 1000 of neutron-rich nuclides with neutron numbers near $N = 50$. The overproduced species include, for example, ^{90}Zr, ^{89}Y, and ^{88}Sr. Though the cited calculations are based on the one-dimensional supernova hydrodynamic calculations of Wilson & Mayle (see Meyer et al. 1992; Qian et al. 1993; or Woosley et al. 1994), it is clear that the overproduction problem will also occur in other computations of late-time supernova evolution, such as the two-dimensional smooth particle hydrodynamic calculations of Herant et al. (1992).

In fact, the overproduction problem in the neutrino-heated supernova ejecta can be traced to material that freezes out of NSE at radii of several hundred kilometers at times of order $t_{pb} < 1$ s. This is a time considerably earlier than the epoch of r-process nucleosynthesis. At this early epoch there has not yet been sufficient time for neutrino interactions to increase the entropy much beyond about $s/k \approx 50$. As a consequence, the baryons at this epoch, and at large enough radii, can reside mostly in alpha particles and heavy iron-peak nuclei.

In the limit where all neutrons and protons are inside alpha particles and heavy nuclei, the neutron-to-proton ratio, n/p, could only change with time as a result of ν_e and $\bar{\nu}_e$ capture processes on nuclei:

$$\nu_e + A(Z, N) \rightarrow A(Z + 1, N - 1) + e^- \, , \tag{3a}$$

$$\bar{\nu}_e + A(Z, N) \rightarrow A(Z - 1, N + 1) + e^+ \, , \tag{3b}$$

where Z is the nuclear charge of the parent nucleus and N is the neutron number, and $A = Z + N$ is the nuclear mass number. As we shall see, charged current neutrino capture rates on alpha particles will be negligible compared to capture rates on nuclei with allowed Fermi or Gamow-Teller strength.

In any case, material flowing out from the vicinity of the neutrino sphere at $t_{pb} \approx 0.5$ s first will be in the form of free nucleons. Y_e will then at first be set by neutino interactions on these species. As the material flows to larger radii, nucleons will assemble into alpha particles with some residual free neutrons. Y_e will shift because of neutrino interactions on these free neutrons. At even larger radii and lower temperature, the mass fraction of free nucleons and alpha particles will decrease and the mass fraction of heavy nuclei will increase. The reactions in equations (3a) and (3b) will then affect Y_e.

The rates for the neutrino capture processes in equations (3a) and (3b) currently are neglected in calculations of neutrino-heated supernova ejecta. Moreover, the processes in equations (1a) and (1b) are included in the supernova models that give the initial conditions for the nucleosynthesis, but have been until now neglected in the nucleosynthesis calculations themselves. In this paper we will argue that inclusion of electron neutrino capture rates on nucleons and heavy nuclei may reduce the neutron excess of nuclei ejected from $t_{pb} < 1$ s and may go at least part of the way toward "curing" the $N = 50$ peak overproduction problem. We will also argue that, in driving the material at this epoch closer to the $Z = N$ line, ν_e captures on free nucleons and heavy nuclei will produce conditions conducive to the NSE-freezeout nucleosynthesis of ^{92}Mo and perhaps some of the other light p-process nuclei.

In what follows, we will give a detailed exposition of the nuclear physics underlying the processes in equations (3a) and (3b). Our treatment is complementary to that of Nadyozhin & Panov (1993) in that we estimate rates of neutrino capture on heavy nuclei. Nadyozhin & Panov (1993), however, only studied the effects of neutrino capture on r-process nucleosynthesis. We go further and, in addition to the above considerations, point out that aspects of nuclear physics make for considerable simplification in the calculations of rates on nuclei of interest in the r-process. In particular, we show that the rates for the processes in equation (3a) become relatively slowly varying functions of Z and N compared to the competing β^--decay rates of importance to the r-process. This property, together with the demand that r-process nucleosynthesis calculations reproduce the observed closed-shell peaks in the solar system heavy element abundance distribution, leads us to a constraint on the location and/or conditions for the site of r-process nucleosynthesis in supernovae.

In § 2 we discuss the physics of electron neutrino and antineutrino capture on nuclei. In § 3 we examine the expected effects of inclusion of our rates on nucleosynthesis from $t_{pb} \lesssim 1$ s, while in § 4 we discuss the effects of these rates on the r-process. We give conclusions in § 5.

2. NEUTRINO CAPTURE ON NUCLEI

In this section we discuss the physics of ν_e and $\bar{\nu}_e$ capture on heavy nuclei in the context of the post–core bounce supernova environment. Our goal is to find simple estimates for the rates of the processes in equations (3a) and (3b) which can be employed in studies of nucleosynthesis from neutrino-heated supernova ejecta.

There are two principal aspects of the calculations of neutrino and antineutrino capture in the post–core bounce supernova environment. First, every capture process has a phase space factor which depends on the local neutrino distribution function, the local electron or positron distribution function, the local matter temperature, and the nuclear Q-value for the weak transition in question. Section 2.1 presents a detailed development of phase space issues for neutrino-induced transitions proceeding at locations above the neutrino sphere. Second, in calculations of neutrino and antineutrino capture cross sections and rates, the distribution of weak strength (Fermi, Gamow-Teller, and forbidden) with nuclear excitation

energy in the parent and daughter nuclei must be estimated. The relevant nuclear physics of these weak strength distributions is discussed in § 2.2.

In what follows, we will show that neutrino and antineutrino capture cross sections and rates in the region above the neutrino sphere can be simply written as a product of a geometrical flux factor Γ (akin to the "dilution factor" employed in studies of photon transport in stellar atmospheres), an effective weak strength ft-value, and a phase space factor. Since our discussion of these ingredient quantities is very detailed, we can suggest an efficient strategy for an initial reading of this paper. First, the reader should examine § 2.1 fairly carefully to get an idea of how the rates are constructed and what form the phase space factors take for various cases. Once the reader has a feeling for this aspect of the problem, § 2.2 on weak strength in nuclei could be skimmed over. This section and its references could be consulted in detail later, when specific rates or cross sections are desired.

Section 2.3 gives three specific examples of the calculations of neutrino and antineutrino capture rates and cross sections. The examples presented are for neutrino-mediated weak transitions occurring in (1) the free nucleons; (2) the $^{56}\mathrm{Fe} \rightleftharpoons {}^{56}\mathrm{Mn}$ system; and (3) nuclei with a large enough neutron excess to be "blocked." On a first reading of this paper, these examples can be consulted to get an idea of how to apply the formulae of § 2.1. To facilitate use of this paper, we provide two tables of symbols and variables. Table 1 presents various physical quantities employed in this work, together with symbols and a brief explanation or label. Table 2 presents quantities used in our expressions for neutrino and antineutrino rates and cross sections. This table also provides a brief explanation for the symbols used for these quantities and some example or defining equation numbers indicating where these quantities are discussed in the text.

TABLE 1

PHYSICAL QUANTITIES

Quantity	Explanation
k	Boltzmann's constant
c	Speed of light in vacuum
L_ν	Neutrino (or antineutrino) energy luminosity
T_ν	Neutrino (or antineutrino) temperature
T_e	Local matter temperature
r_7	Distance from neutron star core in units of 10^7 cm
E_i	Excitation energy for nuclear level i
J_i	Spin of nuclear level i
Q_n^{ij}	Nuclear Q-value for $i \rightarrow j$ nuclear transition
m_e	Electron mass
$\langle G \rangle$	Coulomb wave correction factor
α_Q	Quenching factor ($\alpha_Q \approx \frac{1}{2}$)

2.1. *Total Rates and Cross Sections*

As a preliminary, we should point out that, wherever neutrino capture on nuclei is important in the post–core bounce supernova environment, the plasma temperature (temperature of the electrons and positrons) will be small compared to the temperatures which characterize the distributions of ν_e and $\bar{\nu}_e$. For example, at about $t_{\rm pb} \approx 1$ s the temperatures for the ν_e and $\bar{\nu}_e$ distributions at the neutrino sphere are $kT_{\nu_e} \approx 4.3$ MeV and $kT_{\bar{\nu}_e} \approx 5.3$ MeV, respectively, while the plasma temperature at a radius of roughly 100 km is $kT_e \approx 300$ keV (see Fuller et al. 1992). This implies that we can usually (but not always!) neglect the reverse processes of electron and/or positron capture in equations (3a) and (3b).

In general, the distribution functions for ν_e and $\bar{\nu}_e$ at any location above the neutrino sphere will not be isotropic. However, numerical supernova model calculations show that these distribution functions are nearly thermal in character, with chemical potentials near zero (see Qian et al. 1993, and references therein). In this paper we will adopt a thermal distribution for each neutrino species, though our results can be generalized to arbitrary distributions in obvious manner. Here we follow the prescription of Qian & Fuller (1995) for the treatment of neutrino fluxes above the neutrino sphere. We can approximate the differential number flux, $d\phi_\nu$, for a neutrino species as

$$d\phi_\nu = \frac{d^2\phi_\nu}{dE_\nu\, d\Omega_\nu}\, dE_\nu\, d\Omega_\nu = \frac{1}{8\pi^3}\frac{c}{(\hbar c)^3}\frac{E_\nu^2\, dE_\nu}{\exp\left[(E_\nu - \mu_\nu)/kT_\nu\right] + 1}\, d\Omega_\nu\,, \qquad (4)$$

where c is the speed of light, $\hbar$ is Planck's constant divided by 2π, E_ν is the neutrino energy, μ_ν is the neutrino chemical potential for a neutrino species at its appropriate neutrino sphere (hereafter, we will take $\mu_\nu \approx 0$), T_ν is the temperature of this neutrino species at its appropriate neutrino sphere, and $d\Omega_\nu$ is a differential solid angle, or pencil of directions, for neutrinos of energy E_ν.

As a point at radius r above a neutrino sphere of radius R_ν we can calculate the total energy-differential flux of neutrinos

TABLE 2

QUANTITIES USED IN NEUTRINO CAPTURE RATE EXPRESSIONS

Quantity	Explanation	Relevant Equations
λ	Total rate for ν-induced transition per nucleus	21
P_i	Population index for nuclear level i	22
λ_{ij}	Rate (s^{-1}) for ν-induced transition from nuclear state $i \rightarrow j$	17a
$\mathscr{Z}$	Matter-temperature-dependent nuclear partition function	23
Γ	Geometrical flux factor	17b
Λ_{ij}	Nuclear rate factor (no threshod case: $\xi_n^{ij} \geq m_t$ and $\eta_L = 0$)	18
Λ_{ij}	Nuclear rate factor (threshold case: $\xi_n^{ij} < m_t$ and $\eta_L = -\xi_n^{ij} + m_t$)	19a–19e or 20
ξ_n^{ij}	Temperature-scaled nuclear Q-value for $i \rightarrow j$ transition	16a
m_t	Temperature-scaled electron mass	16b
η_L	Temperature-scaled threshold energy	16d
$\langle ft_{ij} \rangle$	$\langle ft \rangle$-value for $i \rightarrow j$ transition	27a–27b
$\lvert M_{\rm F} \rvert^2$	Square of Fermi matrix element	29
$\lvert M_{\rm GT} \rvert^2$	Square of Gamow-Teller matrix element	33a, 33b, and 34

of a given species with energy E_ν by integrating over the allowed solid angle,

$$d\phi_\nu = \frac{d\phi_\nu}{dE_\nu}\, dE_\nu \approx \frac{1}{8\pi^3}\,\frac{c}{(\hbar c)^3}\,\frac{E_\nu^2\, dE_\nu}{\exp\,(E_\nu/kT_\nu) + 1}\int d\Omega_\nu\,. \quad (5)$$

Anywhere above the neutrino sphere, the flux for any neutrino species will exhibit azimuthal symmetry. However, there will be a maximum polar angle θ_0 for direction pencils which can contribute to the integral over solid angle in equation (5). This maximum polar angle is given by the angle of the limb of the neutrino sphere as seen from a position at radius r. We can write

$$\int d\Omega_\nu = 2\pi(1 - \cos\,\theta_0)\,, \quad (6a)$$

where

$$\cos\,\theta_0 = \sqrt{1 - \frac{R_\nu^2}{r^2}} \approx 1 - \frac{1}{2}\,\frac{R_\nu^2}{r^2}\,. \quad (6b)$$

The approximation in equation (6b) follows whenever $r \gg R_\nu$. This limit will nearly always be applicable at the locations where neutrino or antineutrino capture on nuclei is important. For example, the neutrino sphere has a radius of order $R_\nu \approx 15$ km at $t_{\rm pb} \approx 1$ s, while the region where neutrino capture on heavy nuclei is significant at this epoch is located at radii $r \gtrsim 100$ km. With this approximation, the total energy-differential number flux for a neutrino species with energy E_ν is

$$d\phi_\nu = \frac{d\phi_\nu}{dE_\nu}\, dE_\nu \approx \frac{1}{8\pi^2}\,\frac{c}{(\hbar c)^3}\,\frac{R_\nu^2}{r^2}\,\frac{E_\nu^2\, dE_\nu}{\exp\,(E_\nu/kT_\nu) + 1}\,. \quad (7)$$

For the purposes of calculating neutrino capture rates, it will prove convenient to express the number flux at radius r for each neutrino species in terms of its neutrino sphere temperature, T_ν, neutrino sphere radius, R_ν, and neutrino luminosity, L_ν. Expressing rates in terms of neutrino luminosity is useful, since in most numerical supernova models at late times, the neutrino luminosities become roughly equal for all neutrino species. The total number flux, Φ_ν, at radius r for a neutrino species is the integral over energy of the energy-differential number flux, $d\phi_\nu$,

$$\Phi_\nu = \int d\phi_\nu \approx \frac{c}{8\pi^2(\hbar c)^3}\,\frac{R_\nu^2}{r^2}\,(kT_\nu)^3 F_2(0)\,, \quad (8a)$$

while the corresponding neutrino luminosity is

$$L_\nu \approx 4\pi r^2\left[\frac{c}{8\pi^2(\hbar c)^3}\,\frac{R_\nu^2}{r^2}\,(kT_\nu)^4 F_3(0)\right]. \quad (8b)$$

In these expressions $F_2(0)$ and $F_3(0)$ are the rank 2 and rank 3, respectively, relativistic Fermi integrals of argument zero. We will define the Fermi integral of order k and argument η to be

$$F_k(\eta) \equiv \int_0^\infty \frac{x^k}{\exp\,(x - \eta) + 1}\, dx\,. \quad (9)$$

A useful estimate for the number flux of a neutrino species is then

$$\Phi_\nu \approx 1.58 \times 10^{41}\ {\rm cm^{-2}\ s^{-1}}\left(\frac{L_\nu}{10^{51}\ {\rm ergs\ s^{-1}}}\right)\left(\frac{\rm MeV}{kT_\nu}\right)\frac{1}{r_7^2}\,, \quad (10)$$

where r_7 is the radius in units of 100 km (10^7 cm). During the r-process epoch ($t_{\rm pb} \sim 10$ s), the luminosity for each neutrino species is roughly $L_\nu \approx 10^{51}$ ergs s^{-1} in the Wilson & Mayle calculations (see Qian et al. 1993 or Woosley et al. 1994). At earlier times ($t_{\rm pb} < 1$ s), where p-process nucleosynthesis products might originate, the characteristic neutrino luminosities are $L_\nu \sim 10^{52}$ ergs s^{-1}.

Consider the rate, λ_{ij}, of electron neutrino or antineutrino capture from the ith excited state of a parent nucleus to the jth excited state of a daughter nucleus. Following Fuller, Fowler, & Newman (1980, 1982a, b, 1985, hereafter FFN I, II, III, and IV, respectively), we can write this rate as

$$\lambda_{ij} = \frac{\ln 2}{\langle ft_{ij}\rangle} f_{ij} = \int_0^\infty \sigma_{ij}(E_\nu) d\phi_\nu\,, \quad (11)$$

where $\langle ft_{ij}\rangle$ and f_{ij} are the effective ft-value and phase space factor, respectively, for the weak transition between nuclear parent level i and nuclear daughter level j, and where $\sigma_{ij}(E_\nu)$ is a neutrino energy-dependent capture cross section for this transition.

In turn, the energy-dependent cross section for this transition could be expressed as

$$\sigma_{ij}(E_\nu) \approx \langle G\rangle\,\frac{\ln 2}{\langle ft_{ij}\rangle}\left[\frac{2\pi^2(\hbar c)^3}{c}\right](m_e c^2)^{-5}(Q_n^{ij} + E_\nu)^2\,, \quad (12)$$

where m_e is the electron rest mass, $\langle G\rangle$ is an average Coulomb wave correction factor, and Q_n^{ij} is the *nuclear* Q-value for this transition.

The Coulomb wave correction factor employed here is the one defined in FFN I and Fuller (1982):

$$G(\pm Z, E_e) \equiv \frac{p_e}{E_e}\,F(\pm Z, E_e)\,, \quad (13)$$

where p_e is the final state electron or positron momentum for neutrino capture (eq. [3a]) or antineutrino capture (eq. [3b]), respectively, and where the total final state lepton energy is $E_e = (p_e^2c^2 + m_e^2c^4)^{1/2}$. In equation (13), $F(\pm Z, E_e)$ is the so-called Fermi factor, familiar from standard treatments of the electron spectrum in ordinary beta decay (see FFN I). In this expression, the minus (plus) sign in the argument is chosen for neutrino (antineutrino) capture.

We have factored an average value of G out of the energy-dependent phase space factor for convenience. This procedure gives an adequate treatment of the effects of Coulomb wave correction for cases where final state electrons (positrons) are relativistic (FFN I; Fuller 1982). In turn, given the large average energies of neutrinos in the post–core bounce supernova environment, we expect final state leptons to be relativistic for all nuclear transitions of interest except those near threshold. We shall see later than the relativistic Coulomb wave correction factor gives a small enhancement in the rates and cross sections of neutrino capture reactions on heavy nuclei.

The nuclear Q-value for the transition between nuclear parent state i with excitation energy E_i and nuclear daughter state j with excitation energy E_j is

$$Q_n^{ij} = M(Z, N) - M(Z \pm 1, N \mp 1) + E_i - E_j\,, \quad (14)$$

where the *nuclear* masses of a parent nucleus with Z protons and N neutrons and a daughter nucleus with $Z \pm 1$ protons and $N \mp 1$ neutrons are $M(Z, N)$ and $M(Z \pm 1, N \mp 1)$, respectively. The upper signs are chosen for a weak transition induced by ν_e capture (eq. [3a]), while the lower signs obtain

for $\bar{\nu}_e$ capture (eq. [3b]). Note that the Q-value for ν_e capture for a transition from $i \rightarrow j$ is equal in magnitude, but opposite in sign, to the Q-value for $\bar{\nu}_e$ capture for the reverse transition, $j \rightarrow i$.

Employing the approximate energy-differential neutrino number flux from equation (7), the energy-dependent cross section from equation (12), and including final state lepton phase space blocking, the transition rate λ_{ij} can be written

$$\lambda_{ij} \approx \langle G \rangle \frac{\ln 2}{\langle ft_{ij} \rangle} \left(\frac{R_\nu^2}{4r^2} \right) \frac{1}{(m_e c^2)^5} \int_{E_{\rm TH}}^{\infty} E_\nu^2 (Q_n^{ij} + E_\nu)^2 \times \frac{1}{\exp\,(E_\nu / kT_\nu) + 1} B_e(E_\nu) dE_\nu \,. \quad (15a)$$

In this expression $E_{\rm TH}$ is the neutrino or antineutrino capture threshold energy for transition $i \rightarrow j$,

$$E_{\rm TH} = \begin{cases} 0 & \text{for} \quad Q_n^{ij} \geq m_e c^2 \,, \\ -Q_n^{ij} + m_e c^2 & \text{for} \quad Q_n^{ij} < m_e c^2 \,, \end{cases} \quad (15b)$$

while $B_e(E_\nu)$ is a neutrino (antineutrino) energy-dependent blocking factor for final state electrons (positrons):

$$B_e(E_\nu) = 1 - \frac{1}{\exp\,[(E_\nu + Q_n^{ij} - \mu_e)/kT_e] + 1} \,, \quad (15c)$$

with T_e and μ_e the plasma temperature and electron (positron) chemical potential, respectively, at radius r.

Note that, for transition $i \rightarrow j$, the final state lepton energy is $E_e = E_\nu + Q_n^{ij}$ when the entrance channel neutrino or antineutrino energy is E_ν. For the locations at which neutrino or antineutrino capture on heavy nuclei is important, the plasma temperatures and net electron densities are such that the electron chemical potential is generally small (see Fuller et al. 1992; Qian et al. 1993). This, together with the usually large values of E_e encountered, implies that we can set the final state lepton blocking factor to unity, $B_e(E_\nu) \approx 1$, over a wide range of neutrino energy without appreciable loss of accuracy in the evaluation of the phase space factor in equation (15a). McLaughlin & Fuller (1996) have examined the effect of final state lepton blocking on neutrino capture rates in the post–core bounce supernova environment and find generally small differences from the results presented here.

Since the only dimensions which survive cancellation in equation (15a) come from $\langle ft_{ij} \rangle$, which by convention has the dimensions of time, it proves convenient to measure all energies in units of kT_ν. Therefore, we make the following definitions:

$$\xi_n^{ij} \equiv \frac{Q_n^{ij}}{kT_\nu} \,; \quad (16a)$$

$$m_t \equiv \frac{m_e c^2}{kT_\nu} \,; \quad (16b)$$

$$\eta_\nu \equiv \frac{E_\nu}{kT_\nu} \,; \quad (16c)$$

$$\eta_L \equiv \frac{E_{\rm TH}}{kT_\nu} \,. \quad (16d)$$

With these definitions we can approximate the neutrino or antineutrino capture rate for transition $i \rightarrow j$ as a product of a "geometrical" factor and a "nuclear" factor:

$$\lambda_{ij} \approx \Gamma \Lambda_{ij} \,. \quad (17a)$$

The dimensionless geometrical factor, Γ, depends on the neutrino (antineutrino) temperature at the neutrino sphere, the neutrino (antineutrino) sphere radius, and the radius at which the capture rate is to be evaluated,

$$\Gamma \equiv \left(\frac{R_\nu^2}{4r^2} \right) \left(\frac{kT_\nu}{m_e c^2} \right)^5 \approx (12.679) \left(\frac{L_\nu}{10^{51}\ \text{ergs s}^{-1}} \right) \left(\frac{kT_\nu}{\text{MeV}} \right) \frac{1}{r_7^2} \,, \quad (17b)$$

where, in the last approximation, we have used the relations from equations (8a) and (8b) and subsumed the neutrino sphere radius and four powers of kT_ν into the neutrino (antineutrino) luminosity. The nuclear factor, Λ_{ij}, has the dimensions of a rate and is given by

$$\Lambda_{ij} \equiv \langle G \rangle \frac{\ln 2}{\langle ft_{ij} \rangle} \int_{\eta_L}^{\infty} \eta_\nu^2 (\xi_n^{ij} + \eta_\nu)^2 \frac{1}{e^{\eta_\nu} + 1} d\eta_\nu \,, \quad (17c)$$

where we have neglected the effects of final state electron (positron) phase space blocking.

The phase space factor in equation (17c) can be reduced to a sum of the products of relativistic Fermi integrals and polynomials in powers of the quantities in equations (16a)–(16d). We can identify two cases: the no threshold case, for which $Q_n^{ij} \geq m_e c^2$ and $\eta_L = 0$; and the threshold case, for which $Q_n^{ij} < m_e c^2$ and $\eta_L = -\xi_n^{ij} + m_t$. For the no threshold case, we can write

$$\Lambda_{ij} = \langle G \rangle \frac{\ln 2}{\langle ft_{ij} \rangle} [F_4(0) + 2\xi_n^{ij} F_3(0) + (\xi_n^{ij})^2 F_2(0)] \,, \quad (18)$$

where $F_4(0) \approx 23.33025$, $F_3(0) \approx 5.68219$, and $F_2(0) \approx 1.80300$. The nuclear factor for the threshold case is

$$\Lambda_{ij} = \langle G \rangle \frac{\ln 2}{\langle ft_{ij} \rangle} [F_4(-\eta_L) + \alpha_3 F_3(-\eta_L) + \alpha_2 F_2(-\eta_L) + \alpha_1 F_1(-\eta_L) + \alpha_0 F_0(-\eta_L)] \,. \quad (19a)$$

In equation (19a) the polynomials α_3 through α_0 are

$$\alpha_3 \equiv 2(\eta_L + m_t) \,, \quad (19b)$$

$$\alpha_2 \equiv (\eta_L + m_t)^2 + 2\eta_L m_t \,, \quad (19c)$$

$$\alpha_1 \equiv 2\eta_L m_t (\eta_L + m_t) \,, \quad (19d)$$

$$\alpha_0 \equiv (\eta_L m_t)^2 \,. \quad (19e)$$

The Fermi integrals in equation (19a) can be evaluated by standard techniques. FFN IV gives a number of simple expressions for Fermi integrals in various limiting cases. In the limit where $\eta_L \gg 0$, corresponding to large threshold energy, the "nondegenerate" approximation can be made for the Fermi integrals. In this limit $F_k(-\eta_L) \approx k!\, \exp\,(-\eta_L)$, and we can approximate equation (19a) as

$$\Lambda_{ij} \approx \langle G \rangle \frac{\ln 2}{\langle ft_{ij} \rangle} [e^{(\xi_n^{ij} - m_t)} (24 + 6\alpha_3 + 2\alpha_2 + \alpha_1 + \alpha_0)] \,. \quad (20)$$

The total neutrino (antineutrino) capture rate on a nucleus, λ_{ν_e} ($\lambda_{\bar{\nu}_e}$), is calculated by summing over all possible transitions $i \rightarrow j$ and weighting each parent state with an appropriate population index:

$$\lambda_{\nu_e(\bar{\nu}_e)} = \sum_i P_i \sum_j \lambda_{ij} \,, \quad (21)$$

where P_i is the population index,

$$P_i = \frac{(2J_i + 1)e^{-E_i/kT_e}}{\mathscr{Z}} . \quad (22)$$

In equation (22) $\mathscr{Z}$ is the temperature-dependent nuclear partition function,

$$\mathscr{Z} = \sum_i (2J_i + 1)e^{-E_i/kT_e} . \quad (23)$$

At this point it is important to note that instead of calculating the total neutrino (antineutrino) capture *rate*, we could just as well compute the total energy-dependent cross section, $\sigma_{\nu_e}(\sigma_{\bar{\nu}_e})$,

$$\sigma_{\nu_e(\bar{\nu}_e)}(E_\nu) = \sum_i P_i \sum_j \sigma_{ij}(E_\nu) , \quad (24)$$

where the notation is as above, and we take the cross section for each transition in the sum from equation (12). In many numerical supernova evolution calculations it is frequently the cross section which is needed and not the rate. In this paper, however, our arguments about astrophysical effects revolve around rates, and therefore we provide simple approximations for capture rates. It is straightforward to utilize a comparison between equations (21) and (24) to translate our results from rates to cross sections.

2.2. *Weak Strength Distributions in Nuclei*

Because the average neutrino and antineutrino energies in the post–core bounce supernova environment are so large, it turns out that usually only a few transitions will dominate the sums in equations (21) and (24). These are the resonance transitions (FFN II). In fact, the neutrino energies are large enough that the allowed Fermi and Gamow-Teller strength in these resonances can be accessed; but the neutrino energies are not so large that forbidden weak strength is necessarily always dominant. This is a situation similar to that for neutral current neutrino-nucleus processes in supernovae (Haxton 1987; Fuller & Meyer 1991)—forbidden transitions are only guaranteed to dominate when there is no appreciable allowed strength available. In what follows, we will neglect forbidden weak strength contributions, but it is important to keep in mind that when the rates derived on the basis of allowed strength are small, forbidden contributions will become dominant. In any case, the effect of forbidden neutrino-capture channels will always be to *increase* the rates over the allowed estimates presented here, enhancing their astrophysical effects. We are investigating the effects of forbidden weak strength on astrophysical neutrino capture rates, and we are studying the manner in which weak forbidden strength is distributed in nuclear excitation energy (McLaughlin & Fuller 1996; McLaughlin, Fuller, & Meyer 1995).

The vector part of the weak hadronic current in the weak interaction current-current Hamiltonian gives rise to the nuclear Fermi operator,

$$T_\pm = \sum_n \tau_\pm(n) , \quad (25)$$

where the sum runs over all nucleons, n, and $\tau_\pm$ is the isospin raising (+) or lowering (−) operator for individual nucleons. The axial vector part of the weak hadronic current gives rise to the Gamow-Teller operator,

$$GT = \sum_n \boldsymbol{\sigma}(n)\tau_\pm(n) , \quad (26)$$

where again the sum runs over all nucleons, n, and $\boldsymbol{\sigma}$ is the Pauli spin operator for individual nucleons. We designate the absolute squares of the matrix elements of the Fermi and Gamow-Teller operators for transitions between the initial parent and final daughter states as $|M_F|^2$ and $|M_{GT}|^2$, respectively. With the particular choices of the vector and axial vector coupling constants employed in FFN II, the relationship between the Fermi matrix element and the corresponding $\langle ft \rangle$-value for any transition, or sum of transitions, is:

$$\log_{10} \langle ft \rangle \approx 3.791 - \log_{10} (|M_F|^2) . \quad (27a)$$

Analogously, the relationship between the Gamow-Teller matrix element and the corresponding $\langle ft \rangle$-value for any transition, or sum of transitions, is

$$\log_{10} \langle ft \rangle \approx 3.596 - \log_{10} (|M_{GT}|^2) . \quad (27b)$$

The Fermi strength associated with a given level in the parent nucleus essentially is concentrated entirely in the corresponding isobaric analog state in the daughter nucleus. If we define the z-projection of isospin for the parent nucleus to be

$$T_z \equiv \frac{N-Z}{2} , \quad (28)$$

then the absolute square of the total Fermi matrix element for the transition from the ground state of the parent to the first isobaric analog state is

$$|M_F|^2 = T(T + 1) - T_z(T_z \pm 1) = |N - Z| , \quad (29)$$

where $T = |T_z|$ is the total isospin of the parent nucleus, and N and Z refer to the nuclear charge and neutron number, respectively, of the parent. The " − " sign is chosen in equation (29) for neutrino capture, while the " + " sign is chosen for antineutrino capture. There will be non–zero-strength Fermi transitions for neutrino capture on a neutron-rich ($N > Z$) parent nucleus, or antineutrino capture on a proton-rich parent ($Z > N$).

For convenience, we classify the neutrino or antineutrino capture parent nucleus and its corresponding daughter nucleus according to the total isospin of each of their ground states. Of the nuclear transition pair, the one with the larger ground state isospin is designated as the $T^>$ nucleus. The nucleus with the smaller ground state isospin is termed the $T^<$ nucleus. Every $T^>$ nuclear level has a corresponding isobaric analog state in the $T^<$ nucleus.

The excitation energy, E_{IAS}, of the first isobaric analog state in the daughter nucleus is accurately predicted by the Coulomb energy difference between the parent and daughter nuclei. Detailed expressions for E_{IAS} in various cases are given in equations (23) through (26) of FFN II. A simplified, and less general, version of the FFN II results can be given if we define an effective charge, Z', in terms of the nuclear parent charge, Z, as

$$Z' \equiv \begin{cases} Z & \text{for } N \geq Z + 2 \\ Z - 1 & \text{for } N \leq Z - 2 . \end{cases} \quad (30)$$

Where equation (30) is applicable, we can write the excitation energy of the isobaric analog state in the daughter nucleus as

$$E_{IAS} \approx \Delta M_{nuc} \mp \delta m_{np} \pm \frac{6}{5}\frac{Z'e^2}{R_{nuc}} , \quad (31a)$$

where ΔM_{nuc} is the difference between the parent and daughter ground state *nuclear* masses, $\delta m_{np} \approx 1.2934$ MeV is the

neutron-proton bare mass difference, and

$$\frac{6}{5}\frac{Z'e^2}{R_{\rm nuc}} \approx 1.728\left(\frac{Z'}{R_{\rm nuc}}\right) \text{ MeV} , \quad (31b)$$

when the nuclear radius, $R_{\rm nuc}$, is expressed in fermis,

$$R_{\rm nuc} \approx 1.12A^{1/3} + 0.78 . \quad (31c)$$

In equation (31a) the upper signs are chosen for neutrino capture on neutron-rich nuclei, while the lower signs are chosen for antineutrino capture on proton-rich nuclei. Similar expressions for the excitation energy of the isobaric analog state for the cases not represented above (i.e., where, for the parent, $N = Z + 1$ or $Z = N + 1$) can be found in equation (24) and equation (26) in FFN II.

The threshold energy for transitions from the ground state of the parent to the isobaric analog state (for the cases given in eq. [30]) is

$$E_{\rm TH}^{\rm IAS} = -Q_n^{\rm IAS} + m_e c^2 \approx \frac{6}{5}\frac{Z'e^2}{R_{\rm nuc}} + m_e c^2 \mp \delta m_{np} . \quad (32)$$

Again, the upper sign in this equation is for neutrino capture, while the lower sign is for antineutrino capture. It is significant that this threshold energy is *independent* of the nuclear mass of parent and daughter. This renders the entire contribution of the Fermi transitions to the total rate in equation (21) independent of the nuclear masses.

In general, estimating the total amount of Gamow-Teller strength available to a given level of the parent nucleus, as well as the distribution of this strength with daughter nucleus excitation energy, is far more difficult than in the case of the Fermi transitions. The Fermi operator is simply the isospin raising/lowering operator (eq. [25]), which commutes with the strong-interaction parts of the nuclear Hamiltonian. As a result, all the Fermi strength is concentrated in one daughter nucleus energy eigenstate. In contrast, the Gamow-Teller operator (eq. [26]) is proportional to the spin of the nucleon that is making the weak transition. Since the nuclear Hamiltonian is strongly spin dependent, the Gamow-Teller operator will not commute with it, and therefore we expect the Gamow-Teller strength to be spread out over many nuclear daughter states.

We define $S_{\beta+}$ to be the total amount of Gamow-Teller strength available for the $\bar{\nu}_e$-capture–induced transition from the parent nucleus ground state:

$$S_{\beta+} \equiv \sum_f (|M_{\rm GT}|^2)_{if} , \quad (33a)$$

where the initial state, i, is taken to be the parent ground state and we sum over all possible daughter states, f. This is the same transition channel as that induced by electron capture or β^+-decay.

In similar fashion, we define $S_{\beta-}$ to be the total amount of Gamow-Teller strength available in the ν_e-capture–induced transition channel from the parent nucleus ground state:

$$S_{\beta-} \equiv \sum_{f'} (|M_{\rm GT}|^2)_{if'} , \quad (33b)$$

where the initial state, i, is taken to be the parent ground state and we sum over all possible daughter states, f'. In turn, this transition channel is equivalent to that induced by positron capture or β^--decay. The total amount of Gamow-Teller strength in each channel is related to the initial-state parent nucleus charge, Z, and neutron number, N, through the sum rule (Ikeda 1964),

$$S_{\beta-} - S_{\beta+} = 3(N - Z) . \quad (34)$$

Shell model calculations of Gamow-Teller strengths do not in general agree with experimental measurements. There is less experimentally observed strength than calculated strength. The shell model Gamow-Teller strength is said to be "quenched." Furthermore, the quenching reduction factor appears to be relatively uniform with daughter nucleus excitation energy. As revealed in nuclear (p, n) reaction measurements (Goodman et al. 1980), this reduction factor (quenching factor) seems to be between about 40% and 60% for $S_{\beta-}$ strength in nuclei with a neutron excess (see Bloom et al. 1981). Similar quenching factors seem to obtain for the $S_{\beta+}$ strength in these nuclei (see Aufderheide et al. 1993, and references therein; FFN IV).

All Gamow-Teller matrix elements, $|M_{\rm GT}|^2$, and sums of such matrix elements (e.g., $S_{\beta-}$ and $S_{\beta+}$) should be quenched by a uniform quenching factor, which we will define to be α_Q (FFN IV). Since the astrophysical neutrino and antineutrino capture rates are linear in the quantities $|M_{\rm GT}|^2$, $S_{\beta-}$, and $S_{\beta+}$, we will implement quenching in this paper by multiplying all Gamow-Teller contributions, λ_{ij}, in equation (21) by α_Q. Note that any Fermi transitions contributing to the sum in equation (21) should not be quenched. Likewise, rate contributions from transitions between discrete nuclear parent and daughter states for which there are *measured* transition matrix elements (ft-values) should not be quenched. In this paper we shall adopt $\alpha_Q = \frac{1}{2}$ as the quenching factor for neutrino or antineutrino capture processes on heavy nuclei. Clearly, there should be no quenching for capture processes on free neutrons and protons.

The evaluation of $S_{\beta-}$ and $S_{\beta+}$ proceeds according to the isospin projection of the parent nucleus. For a parent nucleus with a neutron excess, $N \geq Z$, electron antineutrino capture tends to be relatively blocked by final nuclear state neutron phase space considerations, while the reverse channel of neutrino capture is relatively less blocked. In this case, we therefore anticipate that $S_{\beta-} \geq S_{\beta+}$, and when the neutron excess is large enough we expect that the $\bar{\nu}_e$-capture channel will be completely blocked and $S_{\beta+} = 0$ (Fuller 1982). In the case of a parent nucleus with a neutron excess, it is simplest to first make an estimate of the usually small amount of $S_{\beta+}$ and then use the sum rule in equation (31) to get an estimate for the usually dominant value of $S_{\beta-}$. The value of $S_{\beta+}$ and its distribution in daughter nucleus excitation energy must be obtained, in most cases, by a shell model calculation. Simple single particle estimates of $S_{\beta+}$ are given in FFN II. A "state of the art" set of shell model calculations for a few cases fit to (n, p)-reaction data, as well as an in-depth discussion of shell model issues, is given in Aufderheide et al. (1993).

In this paper we will estimate the amount of $S_{\beta+}$ strength for nuclei with a neutron excess by using the single-shell model procedure outlined in FFN II. First we adopt a set of shell model single-particle energies for neutrons and protons. For this particular ordering of single particle states, we construct a "zero order" set of single particle occupation numbers for the $\bar{\nu}_e$-capture parent and daughter nuclei. Then we compute the total amount of Gamow-Teller strength using equations (16), (17), and (18) on page 722 of FFN II, and as a by-product we obtain the zero-order configurations of the possible spin-flip states in the daughter nucleus. As described in FFN II, comparison of these spin-flip configurations with the daughter nucleus ground state configuration allows us to make an estimate of the excitation energy centroid of the $S_{\beta+}$ distribution.

The $S_{\beta-}$ strength is then obtained by employing equation (34). Nuclei with a proton excess are treated in an obviously analogous fashion, except that $S_{\beta-}$ is estimated using the FFN II procedure, and $S_{\beta+}$ is obtained from the sum rule in equation (34).

Shell model calculations and a few (n, p) reaction studies (see Aufderheide et al. 1993; Bloom & Fuller 1985) show that the distribution of $S_{\beta+}$ for nuclei with a neutron excess is fairly concentrated in a narrow region of daughter nucleus excitation energy, at least when $S_{\beta+}$ is large enough to make a significant contribution to the total rate. We shall follow FFN II and lump this strength in a "resonance" state. The extensive (p, n)-reaction data show that the $S_{\beta-}$ strength is collected in a true resonance state in the daughter nucleus. We shall again follow FFN II and lump all the $S_{\beta-}$ strength in a single resonance state.

We depict the positions of these reasonance states for a generic case of a neutron-rich parent nucleus in Figure 1. In this figure the ν_e-capture parent nucleus, the $T^>$ nucleus, has nuclear charge Z and neutron number N, while the $\bar{\nu}_e$-capture parent, the $T^<$ nucleus, has nuclear charge $Z + 1$ and neutron number $N - 1$. Arrows show the dominant ν_e-capture channel transitions from the ground state of the $T^>$ parent nucleus to the Fermi resonance (the isobaric analog state, IAS) and the $T^>$ Gamow-Teller resonance state ($T^>$-RES). The $T^>$ Gamow-Teller resonance state is taken to contain the lumped $S_{\beta-}$ strength. The $S_{\beta+}$ strength is lumped in the $T^<$ Gamow-Teller resonance state ($T^<$-RES). This state must be thermally populated in order that a ν_e-capture transition to the $T^<$ nucleus ground state be possible in this model. If we were to reverse the directions of the arrows and consider $\bar{\nu}_e$ capture on a $T^<$ parent nucleus, then the IAS and $T^>$-RES states would have to be thermally populated to give transitions to the ground state of the $T^>$ daughter nucleus in our model.

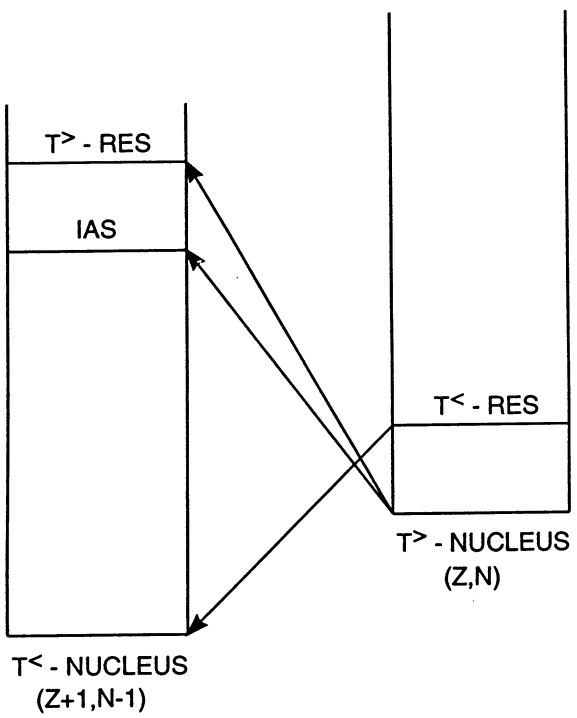

FIG. 1.—"Resonant" ν_e capture transitions are shown from a $T^>$ parent nucleus with Z protons and N neutrons to a $T^<$ daughter nucleus. The isobaric analog state is labeled by IAS, while the Gamow-Teller "collective states" are denoted as $T^>$-RES and $T^<$-RES.

The above discussion can be generalized to the case of a nuclear parent with a *proton* excess in obvious fashion. In this case, for example, $S_{\beta+}$ will generally be larger than $S_{\beta-}$, the $T^<$-RES state will contain the $S_{\beta-}$ strength, while the $S_{\beta+}$ strength will be concentrated in the $T^>$-RES state.

Data from (p, n) nuclear reactions on target nuclei with neutron excesses show that the $T^>$-RES state generally lies a few MeV above the first IAS state. A study by Bertsch & Esbensen (1987) has examined the available experimental data and found that the splitting, or energy difference, δ, between the excitation energy of the IAS, $E_{\rm IAS}$, and the centroid of the Gamow-Teller $T^>$-RES strength distribution, $E_{\rm GT>}$, has a linear dependence on the neutron excess, $(N - Z)/A$, of the parent nucleus. In fact, on theoretical grounds they suggest that this splitting is given by

$$\delta = R_{\rm GT>} - E_{\rm IAS} \approx \Delta E_{\rm es} + 2\left(\frac{\kappa_{\sigma\tau} - \kappa_\tau}{A}\right)(N - Z)\,, \quad (35)$$

where $\Delta E_{\rm es}$ is a parameter related to the Lane potential (see FFN II) and $\kappa_{\sigma\tau}$ and κ_τ are leading coefficients in the effective (Yukawa) potentials for the $\boldsymbol{\sigma\tau} \cdot \boldsymbol{\sigma\tau}$ and $\tau \times \tau$ components of the nucleon-nucleon interaction, respectively. Bertsch & Esbensen (1987) examined and tabulated all known (p, n)-reaction data as of 1987 and suggested that the best fit to this data would be $\Delta E_{\rm es} \approx 3$ MeV and $\kappa_{\sigma\tau} - \kappa_\tau \approx -13.5$ MeV.

We have reexamined the (p, n) reaction data set and we find that, at least for the purposes of calculating ν_e capture rates on neutron-rich nuclei, a better fit to this data gives a splitting (in MeV) between the IAS and the $T^>$-RES centroid as

$$\delta \approx \begin{cases} 54\bar{Y}_e - 20.35 & \text{for } \bar{Y}_e \geq 0.377\,, \\ 0 & \text{for } \bar{Y}_e < 0.377\,. \end{cases} \quad (36a)$$

In this expression the effective electron fraction for a particular nucleus is defined in terms of its charge, Z, and mass number, A, to be

$$\bar{Y}_e \equiv \frac{Z}{A}\,. \quad (36b)$$

Note that with this definition the neutron excess for a nucleus with Z protons and N neutrons is just $(N - Z)/A = 1 - 2\bar{Y}_e$.

There is no simple prescription for estimating the width of the Gamow-Teller $T^>$ resonance. Indeed, some (p, n) reaction data show that this resonance can be very narrow in excitation energy. This seems to be especially true when the target (parent) nucleus has a neutron and/or proton number near that of a closed shell or subshell. This is fortunate, since the nuclei for which the role of ν_e capture is of paramount importance in the r-process are the so-called waiting point nuclei. The waiting point nuclei have small β^--decay rates and serve as choke points in the r-process flow. In turn, the nuclei with the smallest β^--decay rates tend to be those near closed shells. On the other hand, away from closed shells, or when the total Gamow-Teller strength is small, the strength distribution can be very spread out and fractionated among the daughter states (see Aufderheide et al. 1993; Bloom et al. 1981; Bloom & Fuller 1985).

It is important to note that electron neutrino capture on heavy neutron-rich nuclei may generally populate a region of excitation energy in the daughter nucleus (the vicinity of the

IAS or $T^>$-RES state) which is particle unstable. In this case, the resonance will certainly be wide, at least in the sense that particle emission is nearly certain. In nuclear statistical equilibrium (NSE), it may well be that only minimal readjustments in equilibrium abundances result from this process. The situation is not so clear when freezeout from NSE is approached. Particle emission following a charged current weak reaction may have important implications for nucleosynthesis in this regime. For example, ν_e capture on heavy nuclei with $N \approx Z$ may tend to give proton emission in some cases, which might have an interesting influence on nucleosynthesis. These processes may have a "smoothing" effect on the distribution of nuclear abundance yields from neutrino-heated supernova ejecta, though we tend to think that the neutral current neutrino spallation processes will have a larger effect as a consequence of the larger average energies of μ- and τ-type neutrinos. We are investigating the nucleosynthesis effects of neutrino capture-induced particle emission (McLaughlin et al. 1995).

In any case, here we will assume that the Gamow-Teller strength distribution is essentially a delta function in daughter nucleus excitation energy. In most cases this is a good approximation for the particular problem of neutrino or antineutrino capture in the post–core bonce supernova environment, because the average neutrino and antineutrino energies are large compared to typical resonance centroids and widths (McLaughlin & Fuller 1996; McLaughlin et al. 1995). By contrast, solar neutrino capture rates on the heavy nuclei which are candidates for solar neutrino detectors (e.g., ^{127}I) can be very sensitive to the assumed width of the Gamow-Teller resonance (Lutostansky & Shul'gina 1991).

With the above prescriptions, the threshold energy for the transition from the ground state of the parent nucleus to the $T^>$-RES state is

$$E_{\rm TH}^{\rm GT^>} = E_{\rm TH}^{\rm IAS} + \delta = -Q_n^{\rm GT^>} + m_e c^2 \approx \frac{6}{5}\frac{Z' e^2}{R_{\rm nuc}} + m_e c^2 \mp \delta m_{np} + \delta \,, \quad (37)$$

where the upper sign in this expression is for neutrino capture and the lower sign is for antineutrino capture. When $\delta = 0$, the threshold energy for the $T^>$-RES transition is coincident with $E_{\rm TH}^{\rm IAS}$, and is therefore independent of the masses of either the parent or daughter nucleus. From equations (36a)–(36b) it is clear that δ is usually small compared to $E_{\rm TH}^{\rm IAS}$ for neutron-rich nuclei. We can conclude that for these cases $E_{\rm TH}^{\rm GT^>}$ will again be largely determined by the Coulomb energy difference between parent and daughter nuclei.

So far we have considered only those Fermi and Gamow-Teller resonance transitions originating from the ground states of the parent and daughter nuclei (e.g., Fig. 1). We can take account of the corresponding Fermi and Gamow-Teller resonance transitions from the excited states of the parent and daughter nuclei by following FFN II and making a simple modification of the population index, P_i, in the sum in equation (21).

Each state in the $T^>$ nucleus has a corresponding isobaric analog state, or Fermi resonance, in the $T^<$ nucleus. The separation in excitation energy of these Fermi resonance states in the $T^<$ nucleus matches the energy separations of the excited states in the $T^>$ nucleus. Furthermore, the transition matrix elements connecting these states are all the same as that for the transition which connects the ground state to the first isobaric analog state. Here we will assume that Gamow-Teller resonance states work in exactly the same manner as Fermi resonances.

Each excited state with excitation energy E_i in the $T^>$ nucleus will be assumed to have a corresponding $T^>$-RES resonance state in $T^<$ nucleus located at excitation energy E_i above the excitation energy of the first $T^>$-RES state. The first $T^>$-RES state is the Gamow-Teller resonance corresponding to the ground state of the $T^>$ nucleus. Further, we will assume that the Gamow-Teller strength in the resonances corresponding to each of the $T^>$ nucleus excited states is the same as that of the transition from the ground state. These approximations essentially amount to assuming that each excited state has the same Gamow-Teller strength distribution as the ground state, but with the centroid of the strength distribution shifted up by the excitation energy of the parent excited state. This is sometimes called the Brink approximation, in analogy to the similar scaling behavior of the giant dipole resonance. Shell model calculations indicate that the Brink approximation for the Gamow-Teller resonances works fairly well, at least for the iron peak nuclei (Bloom & Fuller 1985; Aufderheide et al. 1993).

As shown in FFN II, employing the Brink approximation allows the sum over the *resonant* Fermi and Gamow-Teller transitions in equation (21) to be replaced by a fully equivalent sum in which the population indices are altered and where the sum runs over only those resonant transitions which connect with either the parent or daughter nucleus ground states. In this FFN II prescription, the direct ν_e-capture–induced transitions from the parent ground state to the IAS and $T^>$-RES states are assigned population factor $P_i = 1$. Similarly, the direct $\bar{\nu}_e$-capture–induced transitions from the parent ground state to the $T^<$-RES state are assigned population factor $P_i = 1$.

However, any transition to the daughter nucleus ground state which proceeds through the thermal population of a Fermi or Gamow-Teller resonance state is assigned a population factor,

$$P_i = \left(\frac{\mathscr{Z}_{\rm daughter}}{\mathscr{Z}_{\rm parent}}\right) e^{-E_i/kT_e} \,, \quad (38)$$

where $\mathscr{Z}_{\rm parent}$ and $\mathscr{Z}_{\rm daughter}$ are the temperature-dependent nuclear partition functions for the parent and daughter nucleus, respectively. In this expression E_i is the excitation energy of the thermally populated resonance state in the parent nucleus. The appropriate excitation energy to employ in equation (38) is chosen as follows: $E_i = E_{\rm IAS}$ for a transition through a thermally populated Fermi resonance; and either $E_i = E_{\rm GT^>}$ or $E_i = E_{\rm GT^<}$ for a transition through a thermally populated $T^>$-RES or $T^<$-RES state, respectively.

Neglecting all discrete state and weak-forbidden transitions, and making the above modifications in the population indices, we can write an approximate expression for the total rate of ν_e capture on the $T^>$ nucleus in Figure 1:

$$\lambda_{\nu_e} \approx \Gamma\left\{\Lambda_{\rm IAS}^{\nu_e} + \alpha_Q\left[\Lambda_{\rm GT^>}^{\nu_e} + \Lambda_{\rm GT^<}^{\nu_e}\left(\frac{\mathscr{Z}^<}{\mathscr{Z}^>}\right) e^{-E_{\rm GT^</kT_e}}\right]\right\} \,, \quad (39a)$$

where $\Lambda_{\rm IAS}^{\nu_e}$ and $\Lambda_{\rm GT^>}^{\nu_e}$ are the nuclear factors for the ν_e capture induced transitions from the ground state of the $T^>$ nucleus parent to the IAS and $T^>$-RES states, respectively. The nuclear

factor for the ν_e capture induced transition through the thermally populated $T^<$-RES state is designated in equation (39a) as $\Lambda^{\nu_e}_{\rm GT<}$. In this equation $\mathscr{Z}^<$ and $\mathscr{Z}^>$ are the temperature-dependent nuclear partition functions for the $T^<$ nucleus and $T^>$ nucleus, respectively.

With the same approximations and notation as in equation (39a), we can estimate the total rate of $\bar{\nu}_e$ capture on the $T^<$ nucleus in Figure 1 to be

$$\lambda_{\bar{\nu}_e} \approx \Gamma\left\{\alpha_Q\left[\Lambda^{\bar{\nu}_e}_{\rm GT<} + \Lambda^{\bar{\nu}_e}_{\rm GT>}\left(\frac{\mathscr{Z}^>}{\mathscr{Z}^<}\right)e^{-E_{\rm GT>}/kT_e}\right] + \Lambda^{\bar{\nu}_e}_{\rm IAS}\left(\frac{\mathscr{Z}^>}{\mathscr{Z}^<}\right)e^{-E_{\rm IAS}/kT_e}\right\}, \quad (39b)$$

where the nuclear factor for the $\bar{\nu}_e$-induced capture transition from the ground state of the $T^<$ nucleus to the $T^<$-RES state is $\Lambda^{\bar{\nu}_e}_{\rm GT<}$, and the nuclear factors for the $\bar{\nu}_e$-induced transitions through the thermally populated IAS and $T^>$-RES states are $\Lambda^{\bar{\nu}_e}_{\rm IAS}$ and $\Lambda^{\bar{\nu}_e}_{\rm GT>}$, respectively. In a straightforward and obvious fashion, we can generalize equations (39a) and (39b) to the case of $\bar{\nu}_e$ and ν_e capture on a nucleus with a *proton* excess.

If, instead of total ν_e or $\bar{\nu}_e$ capture rates, the total neutrino or antineutrino energy dependent cross sections were desired, then the appropriate transition cross sections from equation (12) could be employed in the sum in equation (24) in direct analogy to what is done above. Following this prescription, and with the same approximations as made in equation (39a), we can given the total ν_e energy-dependent cross section for ν_e capture on the $T^>$ nucleus in Figure 1 as

$$\sigma_{\nu_e} \approx \sigma^{\nu_e}_{\rm IAS} + \alpha_Q\left[\sigma^{\nu_e}_{\rm GT>} + \sigma^{\nu_e}_{\rm GT<}\left(\frac{\mathscr{Z}^<}{\mathscr{Z}^>}\right)e^{-E_{\rm GT<}/kT_e}\right], \quad (40a)$$

where $\sigma^{\nu_e}_{\rm IAS}$ and $\sigma^{\nu_e}_{\rm GT>}$ are the ν_e energy-dependent cross sections for the ν_e-capture–induced transitions from the ground state of the $T^>$ nucleus parent to the IAS and $T^>$-RES states, respectively. The corresponding cross section for the ν_e-capture–induced transition through the thermally populated $T^<$-RES state is denoted here as $\sigma^{\nu_e}_{\rm GT<}$.

In like manner, the total $\bar{\nu}_e$ energy-dependent cross section for $\bar{\nu}_e$ capture on the $T^<$ nucleus in Figure 1 is approximately,

$$\sigma_{\bar{\nu}_e} \approx \alpha_Q\left[\sigma^{\bar{\nu}_e}_{\rm GT<} + \sigma^{\bar{\nu}_e}_{\rm GT>}\left(\frac{\mathscr{Z}^>}{\mathscr{Z}^<}\right)e^{-E_{\rm GT>}/kT_e}\right] + \sigma^{\bar{\nu}_e}_{\rm IAS}\left(\frac{Z^>}{Z^<}\right)e^{-E_{\rm IAS}/kT_e}. \quad (40b)$$

In this equation the $\bar{\nu}_e$ energy-dependent cross section for the $\bar{\nu}_e$-induced capture transition from the ground state of the $T^<$ nucleus to the $T^<$-RES state is $\sigma^{\bar{\nu}_e}_{\rm GT<}$, and the corresponding cross sections for the $\bar{\nu}_e$-induced transitions through the thermally populated IAS and $T^>$-RES states are $\sigma^{\bar{\nu}_e}_{\rm IAS}$ and $\sigma^{\bar{\nu}_e}_{\rm GT>}$, respectively. The generalization of equations (40a) and (40b) to the case of neutrino or antineutrino capture on nuclei with a proton excess follows in obvious fashion.

At the high plasma temperatures ($kT_e \approx 300$–600 keV) where neutrino or antineutrino capture on heavy nuclei is important, there is typically little difference in the temperature dependent nuclear partition functions, $\mathscr{Z}^<$ and $\mathscr{Z}^>$, for a nuclear transition pair. For such conditions, the ratios of partition functions in the sums in equations (39a)–(39b) and (40a)–(40b) can be set to unity without appreciable loss of accuracy. A more accurate approximation for these ratios could be obtained by employing the expressions for high-temperature nuclear partition functions in Tubbs & Koonin (1979) and Fowler, Engelbrecht, & Woosley (1978).

All we now require before employing equations (39a)–(39b) and (40a)–(40b) to predict neutrino and antineutrino capture rates and cross sections is a specification of the average Coulomb wave correction factor, $\langle G\rangle$. Fuller (1982) and FFN I give simple estimates of $\langle G\rangle$ for stellar electron capture. The final state electron and positron energies encountered for neutrino and antineutrino capture, respectively, on heavy nuclei can be larger than the typical electron energies considered in Fuller (1982), so that $\langle G\rangle$ should be somewhat smaller for neutrino capture than what was employed in that work. From the considerations in Fuller (1982) and FFN I, we can see that for the neutrino capture problem in this paper $\langle G\rangle \approx 1$–$2$. A complete integration of the phase space factor including the full relativistic Fermi factor suggests that $\langle G\rangle \approx 1.5$ for some of the neutrino capture cases considered here and $\langle G\rangle \approx 0.5$ for the antineutrino capture cases (McLaughlin & Fuller 1995). Given the inherent uncertainties in strength distributions and quenching factors, in the last sections of this paper we shall simply adopt $\langle G\rangle = 2$ for neutrino and antineutrino capture on heavy nuclei. Clearly, $\langle G\rangle \approx 1$ for capture processes on free neutrons and protons.

2.3. *Example Cases*

It is useful at this point to consider several examples. To begin with, consider the neutrino and antineutrino capture reactions on ^{56}Fe and ^{56}Mn,

$$\bar{\nu}_e + {}^{56}{\rm Fe} \rightarrow {}^{56}{\rm Mn} + e^+, \quad (41a)$$

which is a $T^<$ (^{56}Fe) to $T^>$ (^{56}Mn) transition, and

$$\nu_e + {}^{56}{\rm Mn} \rightarrow {}^{56}{\rm Fe} + e^-, \quad (41b)$$

which is a $T^>$ to $T^<$ transition. The reaction in equation (41b) corresponds to the arrow directions in Figure 1, while reversing the arrow directions in this figure would give the case analogous to that in equation (41a).

The first isobaric analog state in ^{56}Fe is predicted by equations (31a)–(31c) to be $E_{\rm IAS} \approx 11.442$ MeV, while equations (36a)–(36b) give $\delta \approx 3.76$ MeV. Using equation (29), we estimate that $|M_{\rm F}|^2 \approx 6$ (or $\log_{10}\langle ft\rangle \approx 3.013$), while the FFN II procedure outlined for computing the excitation energy centroid and total strength for the $T^<$-RES state yields $E_{\rm GT<} \approx 3.777$ MeV and $|M_{\rm GT<}|^2 \approx 72/7 \approx 10.3$ (or $\log_{10}\langle ft\rangle \approx 2.583$) for these quantities, respectively. The total amount of Gamow-Teller strength in the $T^>$-RES state is obtained by estimating S_{β^+} for the ground state of ^{56}Mn using the FFN II procedure and then employing the sum rule in equation (34) to get $|M_{\rm GT>}|^2 \equiv S_{\beta^-} \approx 3 \times 6 + 60.7 \approx 26.6$ (or $\log_{10}\langle ft\rangle \approx 2.171$).

With these parameters, we can use equations (39a)–(39b) to estimate the rates. For example, if we choose $L_{\nu_e} = L_{\bar{\nu}_e} = 3.5 \times 10^{51}$ ergs s^{-1}, $kT_{\nu_e} = 4.3$ MeV, $kT_{\bar{\nu}_e} = 5.3$ MeV, $kT_e = 400$ keV, and $r_7 = 1$, then $\Gamma \approx 190.8$ for the reaction in equation (41b) and $\Gamma \approx 235.2$ for the reaction in equation (41a). For these conditions, the rate of the reaction in equation (41b) is $\lambda_{\nu_e} \approx 7.4$ per nucleus per second, while the rate corresponding to the reaction in equation (41a) is $\lambda_{\bar{\nu}_e} \approx 2.5$ per nucleus per second. This illustrates a general feature of these rates: for typical post–core bounce conditions ν_e capture wins over $\bar{\nu}_e$ capture for nuclei with a neutron excess.

Finally, equations (17a)–(17c) and (18) can be used to make estimates of the discrete state–to–discrete state contributions to the rates of the reactions in equations (41a)–(41b). For the conditions given in the example above, these discrete state transitions give contributions to the rates which fractionally are on the order of $\gtrsim 10^{-4}$ of the rates as calculated with just the resonance transitions using equations (39a)–(39b).

Sufficiently neutron-rich nuclei will be subject to complete neutron Pauli blocking (Fuller 1982) and will therefore have $S_{\beta+} \approx 0$. In this case there will be, for example, no $T^<$-RES state in the $T^>$ nucleus (see Fig. 1), and in the approximations inherent in equation (39b) we would predict $\lambda_{\bar{\nu}_e} \approx 0$. Of course, as discussed in Fuller (1982), there may be some thermal unblocking, as well as a nonzero contribution to $S_{\beta+}$ from forbidden transitions, that results in a nonzero rate. However, for blocked nuclei it will always be the case that $\lambda_{\bar{\nu}_e} \ll \lambda_{\nu_e}$ for the relevant conditions in the post–core bounce supernova environment.

Nuclei will be blocked when there are no allowed single-particle transitions from occupied proton orbits to open neutron orbits. Blocking will occur if, for example, protons are filling the *fp*-shell, while neutrons have completely filled this shell and are filling the *gd*-shell. In this example, blocking obtains when $Z \leq 40$ and $N \geq 40$. There are other, larger, values of Z and N where blocking may occur, depending on the order of the single particle neutron and proton orbits.

For such neutron-rich blocked nuclei, we can give a very much simplified expression for the ν_e capture rate. For a nucleus with proton number Z and neutron number N, we can write approximate ν_e capture rate as

$$\lambda_{\nu_e}(Z, N) \approx \Gamma\{\Lambda_{\rm IAS} + \Lambda_{\rm GTR}\} \quad \text{(BLOCKED)}, \tag{42a}$$

where the Fermi and Gamow-Teller contributions from the IAS and $T^>$-RES states, respectively, are

$$\Lambda_{\rm IAS} \approx \langle G\rangle(1.1216 \times 10^{-4})|N - Z|S_{\rm IAS} \quad \text{(BLOCKED)}, \tag{42b}$$

and,

$$\Lambda_{\rm GTR} \approx \alpha_Q\langle G\rangle(5.2717 \times 10^{-4})|N - Z|S_{\rm GTR} \quad \text{(BLOCKED)}. \tag{42c}$$

In these expressions, $S_{\rm IAS}$ and $S_{\rm GTR}$ are phase space factors given by the functions

$$S_{\rm IAS} \approx e^{-\eta_L^{\rm IAS}}\{(\beta + 6)^2 + [\beta(1 + m_t) - m_t^2]^2 + 4\beta m_t - 4m_t^2 - 12\}, \tag{42d}$$

and,

$$S_{\rm GTR} \approx e^{(-\eta_L^{\rm IAS}+d)}\{(\beta + 6 + d)^2 + [(\beta + d)(1 + m_t) - m_t^2]^2\} + e^{(-\eta_L^{\rm IAS}+d)}[4(\beta + d)m_t - 4m_t^2 - 12]. \tag{42e}$$

In equations (42d)–(42e) the notation is as in equations (16a)–(16d). However, here we can give the threshold for the IAS state corresponding to a neutron shell–blocked parent nucleus as

$$\eta_L^{\rm IAS} \approx \left(\frac{1}{kT_{\nu_e}}\right)\left(\frac{1.728Z}{R_{\rm nuc}} - 0.7824\right), \tag{42f}$$

where $R_{\rm nuc}$ is taken from equation (31c) and kT_{ν_e} is to be expressed in MeV. In the above expressions we define the dimensionless quantity d as

$$d \equiv \frac{\delta}{kT_{\nu_e}}, \tag{42g}$$

and we define β to be

$$\beta \equiv \eta_L^{\rm IAS} + m_t. \tag{42h}$$

The blocked nuclei, for which equations (42a)–(42h) apply, are neutron rich and are characterized by low values of $\bar{Y}_e$. In most cases, blocked nuclei will have $\bar{Y}_e \lesssim 0.377$. As a result, equation (36a) would predict that $\delta \approx 0$ for these cases. In turn, this would imply that for a blocked nucleus $d \approx 0$ and, as a result, the thresholds and phase space factors for the Fermi and Gamow-Teller contributions to the ν_e capture rate in equations (42d)–(42e) would be the same. In this case, the only dependence of the ν_e capture rates on neutron number and proton number comes from the $|N - Z|$ factor in equations (42b)–(42c) and from the fact that the nuclear Q-value is essentially just the Coulomb energy difference between the parent and the daughter nucleus (proportional to Z). The nuclear mass difference does not affect the rate in this case.

The difference of nuclear masses typically is a sensitive function of Z and N resulting from the strong dependence of the nuclear binding energies on shell effects or pairing. As we move across a series of neutron-rich, blocked, nuclear isobars equations (42a)–(42h) predict that the ν_e capture rates will only slowly change from nucleus to nucleus. In contrast, we will find that β^--decay rates may change by several orders of magnitude from nucleus to nucleus, partly since these rates depend on the fifth power of the mass difference between nuclear parent and daughter. Also contributing to the sensitivity of β^--decay rates to Z and N is the fact that the *ft*-values for the few discrete state transitions which determine these rates can vary over orders of magnitude between nuclear pairs.

Finally, ν_e capture on free neutrons (eq. [1a]) and $\bar{\nu}_e$ capture on free protons (eq. [1b]) are processes which represent unique cases of our rate calculation procedure and therefore merit special attention. The rates for these reactions can be calculated using equations (17a)–(17c), (18), and (19a)–(19e). The corresponding cross sections follow from equation (12). The rates for both of the reactions in equations (1a)–(1b) should be calculated using a quenching factor of unity, $\alpha_Q = 1$, and a Coulomb wave correction factor $\langle G\rangle \approx 1$.

The weak transition which mediates the reaction in equation (1a) has $|M_{\rm F}|^2 = 1$ and $|M_{\rm GT}|^2 = 3$, which together imply a total combined *ft*-value of $\log_{10}\langle ft\rangle \approx 3.035$. The neutron and the proton are mirror "nuclei," and therefore the weak transition in equation (1b) has the same matrix elements and overall combined *ft*-value as the transition in equation (1a).

The process in equation (1a) is clearly a no threshold transition and has nuclear Q-value

$$Q_{np}^{\nu_e} = \delta m_{np} \approx 1.2934 \text{ MeV}, \tag{43a}$$

which, in units of the ν_e temperature, is (see eq. [16a])

$$\xi_{np}^{\nu_e} = \frac{Q_{np}^{\nu_e}}{kT_{\nu_e}}. \tag{43b}$$

The reaction in equation (1b) is a threshold transition. The nuclear Q-value for this reaction is

$$Q_{pn}^{\bar{\nu}_e} = -Q_{np}^{\nu_e}. \tag{43c}$$

The threshold for this transition in units of the $\bar{\nu}_e$ temperature is

$$\eta_L = \frac{-Q_{pn}^{\bar{\nu}_e} + m_e c^2}{kT_{\bar{\nu}_e}} \approx \frac{1.8044}{kT_{\bar{\nu}_e}}, \quad (43d)$$

where in the latter approximation we express $kT_{\bar{\nu}_e}$ in MeV. When calculating the rate for the reaction in equation (1b), it is important to recognize that the argument of the Fermi integrals in equation (19a), $-\eta_L$, will be negative but small. Note that the first-order "nondegenerate" approximation for the Fermi integrals may not be adequate when $-\eta_L$ is near zero. In this case, a more accurate and detailed integration of the Fermi integrals is warranted.

The above considerations have provided a simple prescription for the calculation of the ν_e and $\bar{\nu}_e$ capture rates and cross sections on nuclei and free nucelons in the post–core bounce supernova environment. This prescription should suffice for incorporating these weak processes in detailed numerical supernova evolution computations. It is, however, straightforward to predict how inclusion of these rates might affect models of nucleosynthesis in neutrino-heated supernova ejecta.

3. NEUTRINOS AND NUCLEOSYNTHESIS FOR $t_{pb} \lesssim 1.0$ s

Woosley & Hoffman (1992) proposed that the α-process and the *r*-process were freezeouts from nuclear statistical equiliberium (NSE) that occurred in the high-entropy "hot bubble" in Type II supernovae. The high entropy per baryon, s/k (in units of Boltzmann's constant), conditions which obtain in the hot bubble imply that there will be a large abundance of light particles present at the time of charged-particle reaction freezeout. At the same time, Y_e, the electron-to-baryon ratio, could be relatively small ($Y_e \lesssim 0.45$). The high-entropy, neutron-rich material in the hot bubble produces higher mass nuclei than are produced in freezeouts from NSE in less extreme conditions (see, e.g., Meyer 1994 for more on this point). For high enough entropies ($s/k \approx 400$) and low enough Y_e ($Y_e \lesssim 0.37$), the *r*-process can take place. Meyer et al. (1992) were able to show that the hot bubble was indeed an ideal site for the *r*-process.

Subsequent work has clarified the situation. High-entropy winds blow from the surface of the neutron star born in the collapse event (Duncan et al. 1986), and it is in these winds that the *r*-process is likely to occur. The *r*-process nucleosynthesis calculations performed in the context of realistic supernova calculations have shown good agreement between the computed abundance yields and the observed solar system *r*-process abundance distribution (Takahashi et al. 1994; Woosley et al. 1994).

However, there is one serious problem. These models produce too many $N = 50$ nuclei (namely ^{88}Sr, ^{89}Y, and ^{90}Zr) because they eject too much material with $s/k \approx 50$ and $Y_e \approx 0.46$. Such material readily produces the $N = 50$ nuclei. This overproduction problem is so serious that if Type II supernovae produced ^{90}Zr in the amounts predicted by the models, these supernovae could not also be the source of the solar system's ^{16}O! Resolution of this overproduction problem is thus of considerable importance for understanding how and where the solar system's isotopes were made.

One proposed solution to the overproduction problem is that current models are one-dimensional, while in the actual supernova multidimensional effects, namely convection, will be important, at least early in the explosion (Herant et al. 1992; Miller et al. 1993). Convection would tend to wash out entropy gradients and might reduce the average entropy of hot-bubble material. Recent calculations, however, suggest that the $N = 50$ overproduction problem shows up even in multidimensional models.

We suggest instead that part of the solution to the $N = 50$ overproduction problem may be neutrino capture on free nucleons and nuclei during the α-process and the *r*-process. The previous *r*-process calculations have not included this effect. In order to explain how neutrino capture on nuclei might help solve the overproduction problem, we first review briefly how Y_e gets set in the wind material.

Neutrino capture on free nucleons determines Y_e as wind material first leaves the nascent neuton star. Y_e is set by the competition between the Y_e-increasing reaction $\nu_e + n \rightarrow p + e^-$ and the Y_e-decreasing reaction $\bar{\nu}_e + p \rightarrow n + e^+$. Because an approximate steady state between these reactions establishes itself in the wind, Qian et al. (1993) were able to show that

$$Y_e \approx \left(1 + \frac{T_{\bar{\nu}_e}}{T_{\nu_e}}\right)^{-1}, \quad (44)$$

where T_{ν_e} and $T_{\bar{\nu}_e}$ are the temperatures of the electron neutrinos and antineutrinos, respectively. As the newly born neutron star neutronizes, the mean free path of neutrinos decreases relative to that for the antineutrinos. The antineutrino sphere moves closer into the center of the neutron star where the temperature is higher; thus, $T_{\bar{\nu}_e}$ becomes larger than T_{ν_e} and Y_e in the wind material decreases.

Because neutrino and antineutrino capture on alpha particles is almost negligible, the α-process models discussed above (Takahashi et al. 1994; Woosley et al. 1994) have employed as input the Y_e set at the point where the nucleons lock themselves into ^{4}He nuclei. In a real supernova, however, we would expect Y_e to continue to change via neutrino and antineutrino capture on any free nucleons and nuclei. We suspect that it is the neglect of these reactions in the nucleosynthesis models that is to some degree responsible for the overproduction of the $N = 50$ nuclei.

Consider what happens once the bulk of the nucleons assemble themselves into alpha particles. If $Y_e < 0.5$, there must be some residual neutrons. These free neutrons will capture neutinos, thereby increasing Y_e. The free neutron abundance Y_n and the free proton abundance Y_p are

$$Y_n = 1 - Y_e - \tfrac{1}{2}X_\alpha \quad (45a)$$

and

$$Y_p = Y_e - \tfrac{1}{2}X_\alpha, \quad (45b)$$

where X_α is the mass fraction of alpha particles. If we assume neutrino and antineutrino captures occur rapidly enough to establish a steady state equilibrium between the free n/p ratio and the neutrino fluxes, we find analogously to Qian et al. (1993) that

$$Y_e \approx \frac{1 + (1/2)X_\alpha(T_{\bar{\nu}_e}/T_{\nu_e} - 1)}{1 + T_{\bar{\nu}_e}/T_{\nu_e}}. \quad (46)$$

This expression reduces to that in equation (44) if $X_\alpha = 0$. Furthermore, if $X_\alpha = 1$, then $Y_e = 0.5$.

Suppose $kT_{\nu_e} = 4$ MeV and $kT_{\bar{\nu}_e} = 4.89$ MeV. As long as all the nucleons are free, $X_\alpha = 0$ and the steady state value of Y_e is about 0.45. When the temperature drops, however, all the protons and most of the neutrons lock themselves into alpha

particles. In this case, for $Y_e = 0.45$, $X_\alpha = 0.90$. If the steady state for weak interactions on free nucleons continues, equation (46) shows Y_e will then rise to 0.495. Such a large Y_e will not overproduce ^{90}Zr. In this scenario, then, the overproduction of $N = 50$ nuclei results at least in part from the lack of inclusion of neutrino interactions on free nucleons in the nucleosynthesis models.

In fact, the drive toward $Y_e = 0.5$ is even more dramatic than suggested above because any protons produced by neutrino capture on free neutrons will tend to react with neutrons to assemble more alpha particles. This again leaves a neutron excess and further neutrino capture. A true steady state is thus impossible unless X_α actually reaches unity. This will not occur because heavy nuclei eventually start to appear as material moves out to large radii and the temperature falls. The heavy nuclei lock up free nucleons. Now the change in Y_e comes from the processes in equations (3a) and (3b).

The time rate of change of Y_e as a result of neutrino/antineutrino capture on heavy nuclei is given by

$$\frac{dY_e}{dt} = \sum_i (\lambda_{\nu_e,i} - \lambda_{\bar{\nu}_e,i}) \frac{X_i}{A_i}, \tag{47}$$

where $\lambda_{\nu_e,i}$ and $\lambda_{\bar{\nu}_e,i}$ are the neutrino capture and antineutrino capture rates on species i, respectively, X_i is the mass fraction of species i, A_i is the mass number of species i, and the sum is over all species i. If some heavy nucleus, which we designate as species k, dominates the mass ($X_k \approx 1$), the rate of change of Y_e becomes

$$\frac{dY_e}{dt} = \frac{(\lambda_{\nu_e,k} - \lambda_{\bar{\nu}_e,k})}{A_k}. \tag{48}$$

We note first that for nuclei near the $N = Z$ line in the nuclide chart, the neutrino captures and antineutrino captures will tend to balance out, and so the rate of change of Y_e will be small. More important, however, will be the fact that neutrino and antineutrino capture on nucleons inside of nuclei will occur more slowly than in free nucleons. Thus, the change in Y_e due to neutrino capture on heavy nuclei will be less dramatic that on free nucleons. In fact, application of the rate algorithm given in the last section shows that we will probably not ever reach a steady state equilibrium of Y_e mediated by neutrino capture on heavy nuclei; the rates are just too slow for this. On the other hand, these rates are still frequently found to be large enough to compete with strong and electromagnetic interactions when these begin to freeze out of NSE.

If the heavy nuclei are quite neutron rich, neutrino captures will tend to increase Y_e. As the nuclei approach the $N = Z$ line in the nuclide chart, however, antineutrino captures may become important and, in turn, these will reverse the increase in Y_e. Another possible effect is that the heavy nuclei may preferentially absorb residual free neutrons over residual free protons. The excess free protons would capture antineutrinos and thereby decrease Y_e. Once we reach an epoch where the heavy nucleus mass fraction is significant, we will need a nuclear reaction network code to follow the changes in Y_e. Nevertheless, because the neutrino capture on heavy nuclei is less important than on free nucleons, the Y_e change in this epoch should be smaller than the change that occurs during the free particle and alpha particle epoch.

Although neutrino capture on heavy nuclei might not dramatically affect Y_e, such reactions may be a mechanism for enhancing the production of some of the light p-nuclei, particularly ^{92}Mo. Previous models of the p-process have failed to produce the rather abundant light p-nuclei in their solar proportions, especially the Mo and Ru isotopes.

The reason for this failure is fairly straightforward. The gamma process in Type II supernovae (Woosley & Howard 1978) can account for the solar system's abundance of the heavy p-nuclei (e.g., Rayet et al. 1995). In this process, photodisintegration reactions convert heavy seed nuclei (originally produced in the r-process or s-process) into p-nuclei. Since most of the heavy p-nuclei are about a factor of 100 less abundant than the seed nuclei, only 1% of the galaxy's matter needs to have passed through gamma-process conditions in order to have synthesized the heavy p-nuclei. The light p-nuclei, on the other hand, are nearly as abundant as their r-process and s-process counterparts. Any disintegration process that successfully produces the heavy p-nuclei from a solar system seed abundance distribution would underproduce the light p-nuclei by 1 or 2 orders of magnitude.

This argument thus calls for a different mechanism for production of the bulk of the light p-nuclei. Proton captures, along with enhanced light seed abundances, in Type Ia supernova explosions are a proposed mechanism (Howard, Meyer, & Woosley 1991) for light p-nuclei production. This model has not proven as successful as originally hoped, however, in light of realistic calculations of Type Ia explosions (Howard & Meyer 1993). We suggest instead that neutrino captures during the α-process may represent a mechanism for synthesis of the light p-nuclei. Of course, there may be other production channels for the light p-nuclei. Which one, if any, dominates may depend on the detailed history of the shock reheating environment in Type II supernovae. We refer the reader to Lambert (1992) and Meyer (1994) for a review of the p-process.

For low Y_e ($\lesssim 0.475$) and $s/k \approx 50$, the nuclear flow to ^{92}Mo mostly passes through ^{90}Zr, since the latter nuclide is so strongly bound. At the time the abundance of ^{90}Zr builds up in the α-process, however, the only abundant light particles are the alpha particles (although a small abundance of protons is also available). Capture of alpha particles on ^{90}Zr leads to ^{94}Mo, thereby bypassing ^{92}Mo. Furthermore, since ^{90}Zr is so strongly bound and the coulomb barrier is large, the alpha capture beyond ^{90}Zr is minimal. Some production of ^{92}Mo occurs because of proton capture on ^{90}Zr and ^{91}Nb. Woosley & Hoffman (1992) have found production of ^{92}Mo in the α-process by alpha captures for $Y_e \sim 0.46$ with higher entropies. Recent investigations show that the α-process by itself may make satisfactory amounts of ^{92}Mo and other light p-nucleus species, but only if the electron fraction lies within a narrow range at some points during the freezeout process (Hoffman et al. 1995). However, this may be a more viable model for production of the light p-nuclei than that suggested here, especially given the vary large fluence of ν_e and $\bar{\nu}_e$ neutrinos required for neutrino capture to effect the desired result. However, we should point out that there is as yet only a very imperfect understanding of the hydrodynamic and heating history of the supernova environment at $t_{pb} \lesssim 1$ s.

When neutrino captures are included in α-process models, the ^{92}Mo production picture might change dramatically in conditions of high neutrino fluence. For example, ^{90}Zr, beta stable in the laboratory, could capture neutrinos in the supernova environment and thereby effectively suffer a "beta decay." The daughter nucleus ^{90}Nb has a large neutron capture cross section and could capture a neutron to become ^{91}Nb, which is an $N = 50$ nucleus with a small neutron capture

cross section and a large neutron binding energy. Such a reaction sequence can thus build up a considerable supply of ^{91}Nb. A similar neutrino-capture/neutron-capture sequence could produce ^{92}Mo. More precisely, ^{91}Nb could now capture a neutrino to become ^{91}Mo, which subsequently captures a neutron to become ^{92}Mo. Additional production of ^{92}Mo may come from the fact that lighter nuclei also can neutrino capture and become considerably less neutron rich, perhaps even proton rich. These nuclei may then shed their excess protons which can then capture on ^{90}Zr and ^{91}Nb to make ^{92}Mo. Similar types of reactions could make the other p-nuclei, although it is not clear that the production of these other light p-nuclei would be as efficient as that for ^{92}Mo, for which the captures occur on abundant ^{90}Zr.

In order to test the plausibility of our speculations, we included neutrino and antineutrino capture on free nucleons and heavy nuclei in a nuclear reaction network developed by one of us (B. S. M.). The network includes strong and electromagnetic reactions up to tin ($Z = 50$), with rates from Woosley et al. (1975), Thielemann, Arnould, & Truran (1986), Caughlan & Fowler (1988), and Woosley & Hoffman (1992). Weak rates are from FFN I–IV and Klapdor, Metzinger, & Oda (1984). Nuclear masses are from Möller (1991). We assumed the supernova radiated 3×10^{53} ergs in neutrinos, with the luminosity falling exponentially on a 3 s timescale. Each of the six neutrino species (ν_e, $\bar{\nu}_e$, ν_μ, $\bar{\nu}_\mu$, ν_τ, and $\bar{\nu}_\tau$) was taken to have the same luminosity, as indicated by the detailed supernova calculations (Woosley et al. 1994). Thus, the ν_e and $\bar{\nu}_e$ fluxes each carried away $\frac{1}{6}$ of the 3×10^{53} ergs. We took the neutrino temperatures to be $kT_{\nu_e} = 4$ MeV and $kT_{\bar{\nu}_e} = 4.9$ MeV. These numbers are in agreement with those in the detailed models. The nucleosynthesis began with free neutrons and protons at $Y_e = 0.45$. This is consistent with our chosen neutrino temperatures and equation (44).

Rather than tie our calculations to any detailed fluid dynamical model, we chose simply to hold material at a fixed radius. Nevertheless, we forced the density to fall exponentially with time on a 0.04 s timescale. We held the entropy per baryon of the fluid element fixed at $s/k = 50$. Changes in the temperature corresponding to the decrease in density were then computed by assuming that the entropy remained constant. We included $e^+ - e^-$ pairs and allowed them to annihilate during nucleosynthesis. The calculations began 1 s after core bounce at a temperature of 10×10^9 K. While our model may not realistically represent the actual fluid flows during the supernova explosion process, it should nonetheless allow us to explore the effects of neutrino captures on nucleosynthesis.

Table 3 shows the overproduction factors O for each of the 10 most overproduced nuclei in the five cases we considered. In the first case, we turned off all neutino and antineutrino interactions during nucleosynthesis. As expected, the $N = 50$ nuclei were tremendously overproduced. In the second case, we turned on all neutrino and antineutrino charged current interactions and held the material at $R = 300$ km (i.e., 300 km from the center of the nascent neutron star). For this calculation, there was some change of the overproductions. Most notable, perhaps, is the increase in $O(^{90}\text{Zr})$ and the concomitant decrease in $O(^{88}\text{Sr})$ and $O(^{89}\text{Y})$. Here neutrino capture on $N = 50$ nuclei has facilitated the flow of material up the $N = 50$ closed shell to ^{90}Zr. For the third case, $R = 200$ km, there was a large change in the overproduction factors. The $N = 50$ nuclei overproduction factors decreased by at least a factor of 2 from the previous case. The fourth case, $R = 100$ km, shows extremely interesting nucleosynthesis. The production of the $N = 50$ nuclei is down by about 2 orders of magnitude from the non-neutrino case, and the five most overproduced nuclei are the light p-nuclei and ^{70}Ge.

Finally, in order to test the importance of the neutrino and antineutrino captures for light p-nuclei production, we repeated the $R = 100$ km run, but without neutrino and antineutrino captures on heavy nuclei. While the light p-nuclei ^{74}Se and ^{78}Kr were produced in this run, ^{92}Mo was not. We also checked the importance of neutrino captures in the $R = 100$ km run by including all neutrino interactions except neutrino capture on ^{90}Zr. The result was that $O(^{92}\text{Mo})$ dropped by a factor of 5 while the other overproduction factors remained unchanged to within 10%. Clearly, neutrino capture played an important role in ^{92}Mo production in case four.

We can draw some general conclusions from this simple study. Though our calculation "held" material at a fixed radius while it was heated by the neutrino flux, in fact the holding radius should be viewed as a parameter which essentially tells us the amount of neutrino *fluence* received by the material. Since our calculations show a 2 order of magnitude difference in the reduction of ^{90}Zr for the case of a holding radius of 100 km compared to that of a 300 km holding radius, we can conclude that the efficiency of a neutrino capture induced solution to the $N = 50$ overproduction problem is very sensitive to the neutrino fluence. For an adequate solution to the $N = 50$ overproduction problem, we would require that the outflowing neutrino-heated material experience a neutrino fluence similar to what it would have received if it were held at 100 km. From Table 3 it is clear that a holding radius of 200 km or 300 km would provide a fluence which is too small to effect a solution to the overproduction problem. The one-dimensional outflow in the supernova model employed by Woosley et al. (1994) would not provide a high enough neutrino fluence for neutrino capture to have an appreciable effect on the overproduction problem. We would require some alteration of either the supernova velocity field or the neutrino capture cross sections (they would have to be larger due to, for example, forbidden strength) for our suggestion to work. We should point out, however, that we expect the region in the supernova above the neutrino sphere at $t_{pb} \lesssim 1$ s to be convectively unstable (Herant et al. 1992; Miller et al. 1993). It is conceivable then that material caught in eddies may loiter at a small enough radius to provide a large enough neutrino fluence to provide an adequate solution to the overproduction problem.

While our calculations may not be based on a particularly realistic fluid dynamical model, they are extremely suggestive. The model with $R = 100$ km coproduced some of the light p-nuclei and reduced the production of the $N = 50$ nuclei. These results certainly justify further exploration of neutrino capture during the α-process, especially in the context of realistic supernova models. One failing of our models was the lack of production of ^{94}Mo, ^{96}Ru, and ^{98}Ru in any of the cases studied. These nuclei will present challenges to all α-process models in the future. Such models are currently under investigation (Hoffman et al. 1995).

Neutrino capture during the α-process could also enhance the production of radioactive nuclei such as ^{92}Nb ($\tau_{1/2} \approx 3.5 \times 10^7$ yr), ^{97}Tc ($\tau_{1/2} \approx 2.6 \times 10^6$ yr), and ^{98}Tc ($\tau_{1/2} \approx 4.2 \times 10^6$ yr). Since these nuclei would emerge in the ejecta containing α-process and r-process material, we might expect isotopic anomalies in meteoritic samples of the daughters of

TABLE 3

OVERPRODUCTION FACTORS

^AZ	$O(^AZ)$
No Neutrinos	
^{90}Zr	1.21E+07
^{89}Y	4.76E+06
^{88}Sr	4.53E+06
^{86}Sr	7.19E+05
^{72}Ge	2.44E+05
^{87}Sr	2.41E+05
^{82}Kr	2.07E+05
^{84}Kr	1.92E+05
^{66}Zn	1.71E+05
^{85}Rb	1.62E+05
R = 300 km	
^{90}Zr	1.59E+07
^{89}Y	1.68E+06
^{91}Zr	9.36E+05
^{88}Sr	4.35E+05
^{86}Sr	4.05E+05
^{76}Se	3.10E+05
^{66}Zn	2.63E+05
^{70}Ge	2.18E+05
^{82}Kr	2.13E+05
^{72}Ge	2.12E+05
R = 200 km	
^{90}Zr	7.43E+06
^{76}Se	3.63E+05
^{70}Ge	3.13E+05
^{66}Zn	2.77E+05
^{89}Y	2.64E+05
^{74}Se	2.52E+05
^{80}Kr	1.75E+05
^{86}Sr	1.65E+05
^{82}Kr	1.63E+05
^{72}Ge	1.27E+05
R = 100 km	
^{78}Kr	1.59E+06
^{74}Se	6.22E+05
^{84}Sr	6.02E+05
^{70}Ge	2.48E+05
^{92}Mo	2.38E+05
^{91}Zr	2.15E+05
^{67}Zn	1.58E+05
^{90}Zr	1.46E+05
^{69}Ga	1.40E+05
^{65}Cu	1.40E+05
R = 100 km[a]	
^{64}Zn	9.72E+04
^{74}Se	2.18E+04
^{78}Kr	1.64E+04
^{60}Ni	1.29E+04
^{68}Zn	9.55E+03
^{61}Ni	8.77E+03
^{62}Ni	4.95E+03
^{59}Co	4.60E+03
^{63}Cu	4.36E+03
^{58}Ni	3.39E+03

[a] Capture on free nucleons only.

these radioactivities to be correlated with anomalies in α-process and r-process nuclei.

Another interesting meteoritic implication of neutrino captures concerns microdiamonds found in meteorites (Lewis et al. 1987). These microdiamonds show anomalous isotopic abundance patterns of the noble gasses. In particular, zenon is enriched in its light (^{124,126}Xe) and heavy (^{134,136}Xe) isotopes, while krypton is enriched in its heavy (^{86}Kr) isotope but depleted in its light (^{78}Kr) isotope (Lewis, Srinivasan, & Anders 1975; Anders 1988). One interpretation of the diamonds is that they condensed in the ejecta of Type II supernovae and had noble gas atoms implanted into them (Clayton 1989). Such a model asserts that light zenon produced by the gamma process in the oxygen/neon shell of the stellar envelope mixed up into the helium/carbon shell, where the diamonds condensed and the heavy zenon formed (Howard, Meyer, & Clayton 1992; Clayton et al. 1995). The model accounts for the depletion of ^{78}Kr by noting that this isotope is not made in the oxygen/neon shell of Type II supernovae (although Rayet et al. 1995 find in recent calculations that high-mass supernovae are able to synthesize large amounts of ^{78}Kr in the O/Ne shell). In fact, Howard et al. (1992) and Clayton et al. (1995) assumed that the light p-nuclei (including ^{78}Kr) are predominantly made in Type Ia supernovae (Howard et al. 1992).

We must now reexamine this Type II supernova model for the origin of microdiamonds in light of our speculation that ^{78}Kr production is enhanced by neutrino captures in the α-process in Type II supernovae. If mixing occurred between α-process material and the helium/carbon shell material, we would not expect ^{78}Kr depletion in the microdiamonds. Interestingly, the lack of an enrichment of r-process ^{130}Xe in the diamonds suggests that some physical mechanism prevents this mixing, and the Type II supernova origin of the microdiamonds thus remains a viable hypothesis.

Finally, we note that it is important that the material flowing from the neutron star become neutron-rich enough several seconds after bounce to allow the r-process to occur. This should naturally be the case, as the fluid flow changes from confused convection early to a fast-moving, high-entropy ($s/k \gtrsim 100$) wind at later times. This changeover occurs at later epochs because by then the neutrinos have had plenty of time to heat the material above the neutrino sphere. Eventually, the wind material moves out quickly to large radius so the neutrino interactions may freezeout before assembly of nucleons into alpha particles. The neutrino interaction rates will also decrease with time because the neutrino luminosity will fall off on a $\sim$3 s timescale.

4. STEADY BETA FLOW AND CONSTRAINTS ON THE r-PROCESS SITE

Neutrino capture on nuclei provides an additional means for a nucleus to change its charge beyond normal β^--decay. In an intense neutrino flux, such as exists near a proto–neutron star, neutrino capture can in fact dominate β^--decay as the charge-increasing reaction. This speeds up the r-process and alters the resulting abundance pattern. Because typical nuclei present during the r-process are so neutron rich, the S_{β^+} strength is small, and antineutrino capture is negligible.

The form of the abundance distribution emerging from the r-process depends on the dominant charge-increasing reactions. Nuclear β^--decay is strongly dependent on the parent-daughter nuclear mass difference. This, in turn, depends strongly on microscopic effects in nuclei. The result is that β^--decay rates can vary greatly from nucleus to nucleus. In general, nuclei on the r-process path have fast β^--decay rates. On the other hand, the so-called waiting-point nuclei along closed neutron shells β^--decay slowly. The slow β-decay rates cause an abundance build-up at these nuclei during the r-

process, which leads to the peaks in the solar system abundance distribution.

The situation is different if neutrino capture dominates the charge increase of nuclei. As we have seen from § 2, neutrino capture rates in this environment depend essentially only on the parent-daughter coulomb energy difference, not on the parent-daughter nuclear mass difference. The coulomb energy difference varies slowly, and rather smoothly, from nuclide to nuclide, so there is only a slow variation among the nuclides of the neutrino-capture rates. If neutrino capture dominates charge increase, there would be no large abundance buildup at any nuclei during the *r*-process, and the resulting *r*-process abundance distribution would be *featureless*. In other words, there would be no peaks in the abundance distribution of nuclides! That this is clearly not the case informs us that the neutrino flux must have been low enough to allow normal β^--decay to be the dominant charge-increasing reaction.

We can be quantitative in our comparison of β^--decay and neutrino capture. Table 4 compares λ_β, the β^--decay rate for the *r*-process waiting point nuclei, with λ_ν, the neutrino capture rate for $L_{\nu_e} = 5 \times 10^{50}$ ergs s^{-1} and $kT_{\nu_e} = 3$ MeV. These are essentially the conditions found in Woosley et al. (1994) for $t_{pb} \approx 10$ s, at which point the *r*-process is occurring. Of course, the rate λ_ν falls off as r^2, so we have scaled λ_ν in terms of the square of r_7, the radius from the proto–neutron star in units of 10^7 cm or 100 km. The table also lists r_7^{eq}, the radius at which $\lambda_\beta = \lambda_\nu$. If the given nucleus is inside of r_7^{eq}, it increases its charge more rapidly by neutrino capture than by β^- decay.

The β^--decay rates of waiting point nuclei are typically an order of magnitude or so less than the β^--decay rates of nuclei elsewhere on the *r*-process path. Thus, in order to wash out the *r*-process peaks, neutrino capture rates on waiting point nuclei must be 10 times greater than the β^--decay rates. As we see from Table 4, r_7^{eq} is typically between 2 and 2.5 for $N = 82$ nuclei and $L_{\nu_e} = 5 \times 10^{50}$ ergs s^{-1} and $kT_{\nu_e} = 3$ MeV. For this neutrino luminosity and temperature, strong *r*-process peaks will not develop if the *r*-process occurs closer than about 60–80 km from the proto–neutron star. These conclusions would also depend on the neutrino luminosity and temperature. For example, for a neutrino luminosity 2 times greater, the *r*-process would have to occur more than 85–110 km away from the proto–neutron star.

A more stringent constraint on the location of the *r*-process comes about as follows. The *r*-process tends to establish a local steady beta flow (e.g., Kratz et al. 1993). In such a case, for waiting point nuclei with a magic number of neutrons ($N = N_{Mag}$),

$$\frac{Y(Z+1, N_{Mag})}{Y(Z, N_{Mag})} = \frac{\lambda(Z, N_{Mag})}{\lambda(Z+1, N_{Mag})}, \tag{49}$$

where in the present case $\lambda(Z, N)$ is the total charge-increasing rate on nucleus (Z, N) and $Y(Z, N)$ is the abundance of nucleus (Z, N). Since the total rate for charge increase is $\lambda(Z, N) = \lambda_\beta(Z, N) + \lambda_\nu(Z, N)$, we can write

$$\frac{Y(Z+1, N_{Mag})}{Y(Z, N_{Mag})} = \frac{\lambda_\beta(Z, N_{Mag})}{\lambda_\beta(Z+1, N_{Mag})}\left[\frac{1+R(Z)}{1+R(Z+1)}\right], \tag{50}$$

where $R(Z) = \lambda_\nu(Z, N_{Mag})/\lambda_\beta(Z, N_{Mag})$.

When neutrino capture is negligible, $R(Z) = 0$ and the abundances along closed neutron shells are simply in inverse proportion to their β-decay rates. Kratz et al. (1993) have found from measured λ_β values and inferred abundances that such a situation is approximately true for the $N = 50$ and $N = 82$ *r*-process waiting point nuclei. If this is in fact the case, then $R(Z)$ and/or $R(Z+1)$ cannot be large compared to unity. Since $R(Z)$ depends on $1/r^2$, steady beta flow gives us constraints on where the *r*-process can have occurred.

Figure 2 shows the ratio $\Lambda(29, 50)/\Lambda(30, 50)$ and $\Lambda(47, 82)/\Lambda(48, 82)$, where we define $\Lambda(Z, N) = \lambda(Z, N)Y(Z, N)$, as a function of r_7 for $L_{\nu_e} = 5 \times 10^{50}$ ergs s^{-1} and $kT_{\nu_e} = 3$ MeV. In the case of perfect steady beta flow, this ratio should be unity. Within several hundred kilometers of the proto–neutron star, however, we see that the ratios are in fact greater than unity because of the neutrino capture reactions on the magic nuclei ^{79}Cu, ^{80}Zn, ^{129}Ag, and ^{130}Cd. The ratio $\Lambda(29, 50)/\Lambda(30, 50)$ is about 2 at 150 km and about 1.6 at 250 km. If we insist that steady beta flow should hold to within 20% in the Cu-Zn region of the *r*-process path, as indicated by the work of Kratz et al. (1988), we conclude that the abundances along the *r*-process path had to be set outside of about 550 km. If steady beta flow holds to within 20% for the Cd-Ag region, then the abundances along the *r*-process path had to be set outside of about 100 km.

TABLE 4

β^--DECAY RATE–NEUTRINO CAPTURE RATE COMPARISON

Z	N	A	M_P (MeV)[a]	M_D (MeV)[a]	$\lambda_\nu r_7^2$	λ_β[b]	$(\lambda_\nu/\lambda_\beta)r_7^2$	r_7^{eq}
26	50	76	−12.340	−26.091	21.66	27.73	0.78	0.88
27	50	77	−22.480	−38.130	19.51	110.02	0.18	0.42
28	50	78	−36.290	−45.435	17.54	3.35	5.24	2.29
29	50	79	−42.753	−53.820*	15.74	3.59	4.38	2.09
30	50	80	−51.890*	−59.380*	14.09	1.26∼	11.18	3.34
31	50	81	−57.990*	−66.310*	11.97	0.56∼	21.38	4.62
31	52	83	−48.696	−61.140	14.12	2.24	6.30	2.51
45	82	127	−36.656	−49.908	13.33	10.35	1.29	1.14
46	82	128	−46.890	−56.957	12.24	6.03	2.03	1.42
47	82	129	−54.025	−65.457	11.23	4.88	2.30	1.52
48	82	130	−63.119	−70.010*	10.30	3.47∼	2.97	1.72
49	82	131	−68.490*	−77.380*	9.44	2.57∼	3.67	1.92
49	84	133	−59.146	−71.190*	10.15	3.85∼	2.64	1.62

[a] Mass excesses known experimentally (*) from Tuli 1990 or calculated by Möller 1991.

[b] β^--decay rates known experimentally (∼) from Tuli 1990 or calculated by Kratz et al. 1988.

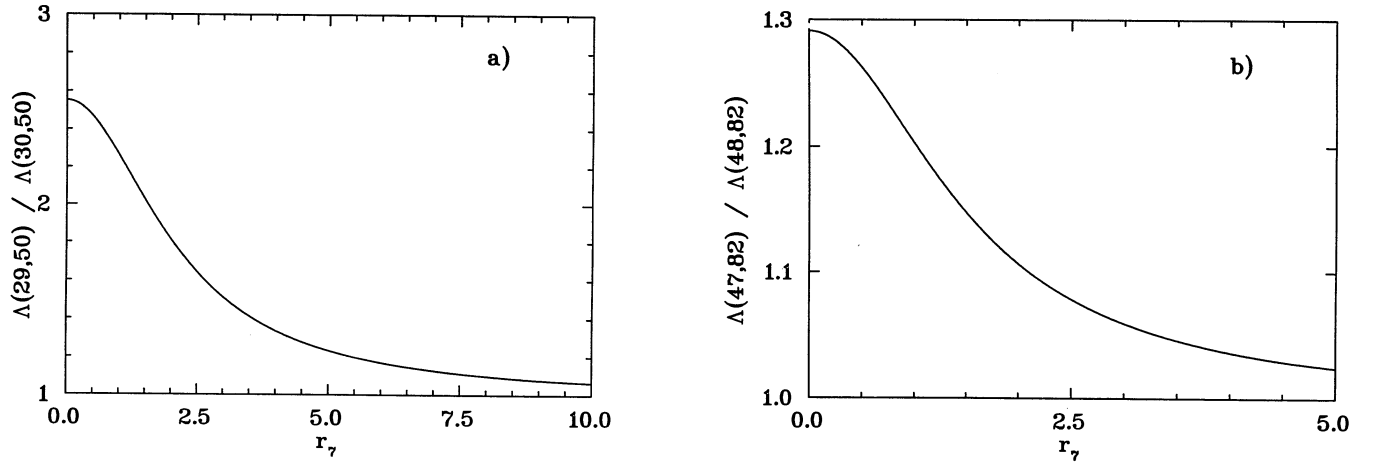

FIG. 2.—The ratio (*a*) Λ(29, 50)/Λ(30, 50) and (*b*) Λ(47, 82)/Λ(48, 82) in steady beta flow as a function of r_7 in the presence of electron neutrinos with a temperature $kT_{\nu_e} = 3$ MeV and a luminosity $L_{\nu_e} = 5 \times 10^{50}$ ergs s^{-1}. When no neutrinos are present, the ratios are unity in perfect steady beta flow.

It is of interest to note that in the models of neutrino-driven winds of Woosley et al. (1994), the freezeout of the *r*-process typically occurs at about 600–1000 km, so this is outside the 550 km limiting radius. It appears, however, that slower wind velocities than are present in Woosley et al. (1994) would lead to *r*-process abundances in contradiction to the Kratz et al. (1988) data.

5. SUMMARY AND CONCLUSIONS

We have estimated neutrino and antineutrino capture rates on heavy nuclei. We have given analytic expressions for these rates to facilitate their inclusion in nucleosynthesis codes. A particularly salient aspect of these rates is that they are dominated by the nuclear transitions to the Fermi and/or Gamow-Teller resonances. This means that the reaction *Q*-value, unlike in the case of nuclear β^--decay, is a smoothly varying function of the parent nucleus proton and neutron number. Also of significance is the fact that antineutrino capture on neutron-rich nuclei will be blocked. Neutron-rich nuclei exposed to an intense flux of neutrinos and antineutrinos will tend to neutrino capture toward the $N = Z$ line in the nuclide chart.

We intend in the future to provide a more detailed treatment of neutrino capture rates on heavy nuclei. We will include discrete nuclear level transitions, better estimates for the location and width of the Gamow-Teller resonance, and the effects of forbidden transitions. Because these improvements will not greatly change our calculations, however, the rate expressions we present in this paper are of sufficient accuracy for inclusion in nucleosynthesis calculations.

When we included our weak interaction rates in α-process calculations near the mass cut of a Type II supernova, we found that they could have a significant effect on the resulting nuclear yields. In particular, for conditions of high neutrino fluxes and/or fluences, neutrino and antineutrino captures on free nucleons and heavy nuclei could solve the $N = 50$ isotope overproduction problem in the α-process and could enhance the production of some of the light *p*-nuclei. However, we found that this mechanism can be effective only if there were considerable modification of the outflow velocity field in existing one-dimensional supernova models.

In another calculation, we were able to use our estimates of neutrino capture rates on heavy nuclei to constrain the site of the freezeout of the *r*-process to a distance of roughly 550 km or more in some cases from the nascent neutron star. In reaching this conclusion, we utilized the fact that neutrino capture alters the nuclear abundances in steady beta flow. This limit on the site of freezeout may prove to be very important for supernova modelers engaged in efforts to understand the late-time neutrino-heated outflow in Type II supernovae.

The effects of neutrino capture during supernova nucleosynthesis will be sensitive to the properties of neutrinos. Tau or μ-type neutrinos with cosmologically significant masses could experience resonant interconversion with electron neutrinos between the neutrinosphere and the region of α-process nucleosynthesis (Fuller et al. 1992). Because the τ neutrinos are more energetic than both the electron neutrinos *and* antineutrinos, resonant interconversion $\nu_\tau/\nu_\mu \rightarrow \nu_e$ would lead to extremely energetic ν_e values. Such conversion would then alter the yields in supernova nucleosynthesis via enhanced neutrino capture. In this way we may ultimately be able to provide tight constraints on the mass difference and mixing angles of massive neutrinos.

The reduction of the overproduction of $N = 50$ isotopes in the α-process and the location of the site of the production of ^{92}Mo are two important problems in nuclear astrophysics. That we may have uncovered important clues to their solutions is an exciting prospect; however, our speculations must be tested by further nucleosynthesis calculations performed in the context of realistic supernova models. Undoubtedly the results of this future work will be quite sensitive to the particular supernova models and neutrino physics employed. This leads to the expectation that the interplay among nucleosynthesis theory, supernova modeling, and particle physics will be strong in the years to come.

We would particularly like to thank Petr Vogel for many illuminating discussions and drawing to our attention to the work of Bertsch & Esbensen. We would also like to thank M. Aufderheide, A. Burrows, D. D. Clayton, R. J. Gould, R. Hoffman, G. C. McLaughlin, Y.-Z. Qian, J. R. Wilson, and S. E. Woosley for useful discussions. This work was supported by an IGPP minigrant, NSF grant PHY 91-21623, and NASA grant NAGW-3480.

REFERENCES

Anders, E. 1988, in Meteorites and the Early Solar System, ed. J. Kerridge & M. Matthews (Tucson: Univ. Ariz. Press), 927
Aufderheide, M. B., Bloom, S. D., Resler, D. A., & Mathews, G. J. 1993, Phys. Rev., C48, 1677
Bertsch, G. F., & Esbensen, H. 1987, Rep. Prog. Phys., 50, 607
Bethe, H. A., & Wilson, J. R. 1985, ApJ, 263, 386
Bloom, S. D., & Fuller, G. M. 1985, Nucl. Phys., A440, 511
Bloom, S. D., Goodman, C. D., Grimes, S. M., & Hausman, R. F. 1981, Phys. Lett., 107B, 336
Burrows, A., & Fryxell, B. A. 1993, ApJ, 418, L33
Caughlan, G. R., & Fowler, W. A. 1988, At. Data Nucl. Data Tables, 40, 283
Clayton, D. D. 1989, ApJ, 340, 613
Clayton, D. D., Meyer, B. S., Sanderson, C. I., Russell, S. S., & Pillanger, C. T. 1995, ApJ, 447, 894
Domogatsky, G. V., & Nadyozhin, D. K. 1977, MNRAS, 178, 33P
Duncan, R. C., Shapiro, S. L., & Wasserman, I. 1986, ApJ, 309, 141
Fowler, W. A., Engelbrecht, C. A., & Woosley, S. E. 1978, ApJ, 226, 984
Fuller, G. M. 1982, ApJ, 252, 741
Fuller, G. M., Fowler, W. A., & Newman, M. J. 1980, ApJS, 42, 447 (FFN I)
———. 1982a, ApJ, 252, 715 (FFN II)
———. 1982b, ApJS, 48, 279 (FFN III)
———. 1985, ApJ, 293, 1 (FFN IV)
Fuller, G. M., Mayle, R., Meyer, B. S., & Wilson, J. R. 1992, ApJ, 389, 517
Fuller, G. M., & Meyer, B. S. 1991, ApJ, 376, 701
Goodman, C. D., Goulding, C. A., Greenfield, M. B., Rapaport, J., Bainum, D. E., Foster, C. C., Love, W. G., & Petrovich, F. 1980, Phys. Rev. Lett., 44, 1755
Haxton, W. C. 1987, Phys. Rev., D36, 2283
Herant, M., Benz, W., & Colgate, S. 1992, ApJ, 395, 642
Hoffman, R. D., Woosley, S. E., Fuller, G. M., & Meyer, B. S. 1995, ApJ, submitted
Howard, W. M., & Meyer, B. S. 1993, in Nuclei in the Cosmos, ed. F. Käppeler & K. Wisshak (Bristol: Institute of Physics), 575
Howard, W. M., Meyer, B. S., & Clayton, D. D. 1992, Meteoritics, 27, 404
Howard, W. M., Meyer, B. S., & Woosley, S. E. 1991, ApJ, 373, L5
Ikeda, I. 1964, Prog. Theor. Phys., 31, 434
Klapdor, H. V., Metzinger, J., & Oda, T. 1984, At. Data Nucl. Data Tables, 31, 81
Kratz, K.-L., Bitouzet, J.-P., Thielemann, F.-K., & Pfeiffer, B. 1993, ApJ, 403, 216
Kratz, K.-L., Thielemann, F.-K., Hillebrandt, W., Möller, P., Härms, V., Wöhr, A., & Truran, J. W. 1988, J. Phys. G, 24, S331
Lambert, D. L. 1992, A&A Rev., 3, 201
Lewis, R. S., Srinivasan, B., & Anders, E. 1975, Science, 190, 1251
Lewis, R. S., Tang, M., Wacker, J. F., & Anders, E. 1987, Nature, 326, 160
Lutostansky, Yu. S., & Shulgina, N. B. 1991, Phys. Rev. Lett., 67, 430
McLaughlin, G. C., & Fuller, G. M. 1995, ApJ, 455, 202
McLaughlin, G. C., Fuller, G. M., & Meyer, B. S. 1995, in preparation
Meyer, B. S. 1993, Phys. Rep., 227, 257
———. 1994, ARA&A, 32, 153
Meyer, B. S., Mathews, G. J., Howard, W. M., Woosley, S. E., & Hoffman, R. 1992, ApJ, 399, 656
Miller, D. S., Wilson, J. R., & Mayle, R. W. 1993, ApJ, 415, 278
Möller, P. 1991, private communication
Nadyozhin, D. K., & Panov, I. V. 1993, in Proc. Int. Symp. on Weak and Electromagnetic Interactions in Nuclei (WEIN-92), ed. Ts. D. Vylov (Singapore: World Scientific), 479
Qian, Y.-Z., & Fuller, G. M. 1995, Phys. Rev., D51, 1479
Qian, Y.-Z., Fuller, G. M., Mathews, G. J., Mayle, R. W., Wilson, J. R., & Woosley, S. E. 1993, Phys. Rev. Lett., 71, 1965
Rayet, M., Arnould, M., Hashimoto, M., Prantzos, N., & Nomoto, K. 1995, A&A, in press
Takahashi, K., Witti, J., & Janka, H.-Th. 1994, A&A, 286, 857
Thielemann, F.-K., Arnould, M., & Truran, J. W. 1986, in Advances in Nuclear Astrophysics, ed. E. Vangioni-Flam et al. (Gif-sur-Yvette: Èditions Frontiéres), 525
Tubbs, D. L., & Koonin, S. E. 1979, ApJ, 232, L59
Tuli, J. 1990, Nuclear Wallet Cards (Brookhaven: Brookhaven National Laboratory)
Woosley, S. E., & Baron, E. 1992, ApJ, 391, 228
Woosley, S. E., Fowler, W. A., Holmes, J. A., & Zimmerman, B. A. 1975, Cal. Inst. Tech., Kellogg Rad. Lab. Preprint No. OAP-422
Woosley, S. E., Hartmann, D. H., Hoffman, R. D., & Haxton, W. C. 1990, ApJ, 356, 272
Woosley, S. E., & Hoffman, R. 1992, ApJ, 395, 202
Woosley, S. E., & Howard, W. M. 1978, ApJS, 36, 285
Woosley, S. E., Mathews, G. J., Wilson, J. R., Hoffman, R. D., & Meyer, B. S. 1994, ApJ, 433, 229